SURFACE ROUGHNESS AND CHIP FORMATION ANALYSIS DURING SINGLE POINT CNC MACHINING OF TITANIUM ALLOY

Author

Ahsen Ali

Regn Number

00000172467

Supervisor

Dr. Hussain Imran

DEPARTMENT OF DESIGN AND MANUFACTURING ENGINEERING

SCHOOL OF MECHANICAL & MANUFACTURING ENGINEERING

NATIONAL UNIVERSITY OF SCIENCES AND TECHNOLOGY

ISLAMABAD

MAY, 2019

SURFACE ROUGHNESS AND CHIP FORMATION ANALYSIS DURING SINGLE POINT CNC MACHINING OF TITANIUM ALLOY

Author

Ahsen Ali

Regn Number

00000172467

A thesis submitted in partial fulfillment of the requirements for the degree of

MS Design and Manufacturing Engineering

Thesis Supervisor:

Dr. Hussain Imran

Thesis Supervisor's Signature: _____

DEPARTMENT OF DESIGN AND MANUFACTURING ENGINEERING

SCHOOL OF MECHANICAL & MANUFACTURING ENGINEERING

NATIONAL UNIVERSITY OF SCIENCES AND TECHNOLOGY

ISLAMABAD

May, 2019

Thesis Acceptance Certificate

Certified that the final copy of MS/MPhil Thesis Written by Ahsen Ali (Registration No: 00000172467), of SMME (School of Mechanical and Manufacturing Engineering) has been vetted by the undersigned, found complete is all respects as per NUST Statutes/ Regulations, is free of plagiarism, errors and mistakes and is accepted as partial fulfillment for award of MS/MPhil Degree. It is further certified that necessary amendments as pointed out by GEC members have also been incorporated in this dissertation.

Signature: _____

Name of the supervisor: Dr. Hussain Imran

Date: _____

Signature (HOD): _____

Date: _____

Signature (Principle): _____

Date: _____

FORM TH-4

National University of Sciences & Technology

MASTER THESIS WORK

We hereby recommend, that the dissertation prepared under our supervision by: (Student Name & Regn No.) **Ahsen Ali & 00000172467** Titled: **Surface Roughness and Chip formation analysis during single point CNC machining of Titanium alloy** be accepted in partial fulfillment of the requirements for the award of **MS Design and Manufacturing Engineering** degree, with (_____) grade.

Examination Committee Members

1. Name: Dr. Mushtaq Khan Signature: _____

2. Name: Dr. Liaqat Ali Signature: _____

3. Name: Dr. Emad-ud-din Signature: _____

Supervisor's name: Dr. Hussain Imran Signature:_____
Date: _____

_____ _____
Head of Department Date

COUNTERSINGED

Date:_____ _____
Dean/Principal

DECLARATION

It is certified that this research thesis titled "*Surface Roughness and Chip formation analysis during single point CNC machining of Titanium alloy"* is my own work. The work has not been presented elsewhere for assessment. The material that has been used from other sources, it has been properly referred.

Signature of Student

Ahsen Ali

2016-NUST-MS-DME-00000172467

PLAGIARISM CERTIFICATE

It is certified that MS Thesis Titled "Surface Roughness and Chip formation analysis during single point CNC machining of Titanium alloy" by Ahsen Ali has been examined by us. We undertake the following:

a) The thesis has significant new work/knowledge as compared already published or are under consideration to be published elsewhere. No sentence, equation, diagram, table, paragraph or section has been copied verbatim from previous work unless it is placed under quotation marks and duly referenced.
b) The work presented is original and own work of the author (i.e. there is no plagiarism). No ideas, processes, results, or words of others have been presented as an Author own work.
c) There is no fabrication of data or results which have been compiled/analyzed.
d) There is no falsification by manipulating research materials, equipment or processes, or changing or omitting data or results such that the research is not accurately represented in the research record.
e) The thesis has been checked using TURNITIN (copy of originality report attached) and found within the limits as per HEC plagiarism Policy and instructions issued from time to time.

Signature of Student

Ahsen Ali

Registration Number

MS-DME-00000172467

Signature of Supervisor

LANGUAGE CORRECTNESS CERTIFICATE

This thesis has been read by an English expert and is free of typing, syntax, semantic, grammatical and spelling mistakes. The Thesis is also according to the format given by the university.

Signature of Student
Ahsen Ali
MS-DME-00000172467

Signature of Supervisor

COPYRIGHT STATEMENT

ACKNOWLEDGEMENT

First and foremost, I am highly thankful to almighty Allah for making be able to accomplish this research work because without his help it wouldn't have been possible.

I am grateful to my loving parents for all their support and the way they brought me up and made me able to handle all kinds of pressure and helped me through thick and thin.

I would also like to convey my special thanks to my supervisor Dr Hussain Imran and my co.supervisor Dr. Mushtaq Khan for all the assistance and help throughout my thesis.

I want to pay my special thanks to Muhammad Younus Khan and Umair Rafiq for their help and support. Every single time I hit a road block, they proposed the best solution. Without their help I wouldn't have been able to complete my thesis. I appreciate all their guidance and patience through the course of my thesis.

I am thankful to Dr. Mushtaq Khan, Dr. Liaqat Ali and Dr. Emad-ud-din for being GEC and express my special thanks to DMRC workers for their assistance.

Dedicated to my loving parents, adored siblings and friends whose help and support made it all possible

Abstract

Titanium alloy grade 5 acquires less tool life and poor machinability relative to other materials. Surface roughness is one of the crucial economic factors for the enhancement of the tool wear while machining of the Ti6Al4V. The factors that cause this problem is the type of material to be machined, suitable condition and parameters such as cutting speed, feed rate, and depth of cut during machining the work piece. The research objective is to investigate how to surface roughness and surface finish varies related to distinctive cutting speeds along with varying the tool coatings, as well as to study the chip geometry and characteristics during machining. For this purpose three types of inserts, uncoated, single coated and multi-coated were used and analyze the results by changing tool coating. A recently created topography was researched and compared against references at distinctive cutting conditions. Chip geometry and morphology were believed to provide information about the chip formation mechanism.

Keywords: Ti-6Al-4V, Tool coatings, Chip geometry, Chip morphology, Surface Roughness

Table of Contents

DECLARATION 5

PLAGIARISM CERTIFICATE 6

LANGUAGE CORRECTNESS CERTIFICATE 7

COPYRIGHT STATEMENT 8

ACKNOWLEDGEMENT 9

1 CHAPTER 01 17

1.1 Introduction 17

1.1.1 Project Background: 17

1.1.2 Project Design: 18

1.1.3 Project scope: 20

2 CHAPTER 02 22

2.1 Literature review: 22

2.1.1 Impacts on machinability of titanium properties 22

2.1.2 Previous research on Surface Roughness and Surface integrity: 24

2.1.3 Previous Research on Chips Morphology and Characteristics: 25

3 CHAPTER 03 28

3.1 Methodology: 28

3.1.1 CNC Turning Test: 28

3.1.2 CNC Lathe machine specification. 29

3.1.3 Operational Setup: 30

3.1.4 Cutting Tools: 30

3.1.5 Cutting Parameters: 32

3.2 Surface Roughness (Ra) Analysis 33

3.2.1 Surface Roughness Description: 34

3.2.2 Type A: 35

3.2.3 Type B: 36

3.2.4 Type C: 36

3.3 Length of active tool engagement analysis: 37

3.4 Chip formation analysis: 38

3.4.1 Sample Preparation: 39

3.5 Chip Characterization: 42
3.6 Optical Microscopy: Chip Geometry and Morphology 45
4 CHAPTER 04 52
4.1 Results and discussion: 52
4.1.1 Comparison and analysis of Ra: 52
4.1.2 Comparison of Uncoated, Single and Multi Coated Surface Roughness vs Cutting speed: 54
4.1.3 Cutting Time Analysis: 58
4.1.4 Chips Characterization with Geometric parameters: 58
5 CHAPTER 05 66
5.1 Conclusion and Recommendation: 66
6 References 68
7 Appendices 71
7.1 Appendix A1 71
7.2 Appendix A2 72
7.3 Appendix A3 73
7.4 Appendix A4 74

List of Figures

Figure 1: Area dependence on material/work piece [1].....18
Figure 2: Project design 19
Figure 3: Schematic pathway and flow chart 20
Figure 4: Different zones of chips for single point turning [21] 26
Figure 5: Single point CNC Turning.....27
Figure 6: ML-300 CNC Lathe machine 28
Figure 7: Operational Experiment setup of CNC turning machine, V_c = Cutting speed, f_n = Feed rate, a_p = Depth of cut 30
Figure 8: Tungsten Carbide SANDVIK inserts.....30
Figure 9: Abrasive wear coefficient of different coatings [24].....31
Figure 10: Tungsten Carbide Schematic view 32
Figure 11: Wear map for turning test of Ti-6Al-4V [25]. 33
Figure 12: Surface Roughness Meter.....34
Figure 13: Schematic figure of Surface Roughness meter 35
Figure 14: Chips Morphology at the Insert - Material interface 38
Figure 15: Hydro press Mounting Machine and achieved chips Mold 39
Figure 16: Metkon GRIPO 2V Grinder, Polisher Machine.....40
Figure 17: Mounted graphite pellets with uncoated cross sectional of chips: 41
Figure 18: Mounted graphite pellets with single-coated cross sectional of chips: 41
Figure 19: Mounted graphite pellets with multi-coated cross sectional of chips: 42
Figure 20: Optical Microscopy Analysis.....42
Figure 21: Optical Microscope OPTIKA 600 connected with PC.....46
Figure 22: Serrated section of chip.....46
Figure 23: Adiabatic shear bands, Crack initiation, Secondary shear zone, chip segments localization in the given chip morphology 47
Figure 24: Line Graph for Cutting Speed vs Type A Ra.....52
Figure 25: Line Graph for Cutting Speed vs Type B Surface Roughness 53
Figure 26: Line Graph for Cutting Speed vs Type C Ra 53
Figure 27: Line graph comparison of uncoated, Single and Multi Coated Ra w.r.t Vc.....54
Figure 28: Bar graph comparison of uncoated, Single and Multi Coated Surface roughness vs Cutting speed.....56
Figure 29: Optical microscopy of uncoated inserts with minimum BUE's.....56

Figure 30: Optical microscopy of single-coated inserts with higher BUE's.....57
Figure 31: Optical microscopy of multi-coated inserts with maximum BUE's.....57
Figure 32: Cutting speed vs Cutting time.....58
Figure 33: Height of peaks with different coating vs Cutting Speed Vc where h_{pu}, h_{ps}, h_{pm} are the uncoated, single and multi-coated height of peaks.....59
Figure 34: Height of valley with different coating as a function of Cutting Speed Vc where h_{vu}, h_{vs}, h_{vm} are the uncoated, single and multi-coated height of peaks.....60
Figure 35: Segment ratio with different coating as a function of Cutting Speed V_c.....61
Figure 36: Deformed chip thickness with different coating as a function of Cutting Speed V_c where t_{cu}, t_{cs}, t_{cm} are the uncoated, single and multi-coated equivalent deformed chip thickness. 62
Figure 37: Shear angle Φ with different coating as a function of Cutting Speed Vc where Φ_u, Φ_s, Φ_m are the uncoated, single and multi-coated shear angles.....63
Figure 38: Chip thickness ratio 'r' with different coating as a function of Cutting Speed Vc where r_u, r_s, r_m are the uncoated, single and multi-coated chip thickness ratios. 63
Figure 39: Chip reduction coefficient '1/r' with different coating as a function of Cutting Speed V_c where (1/r)', (1/r)'', (1/r)''' are the uncoated, single and multi-coated coefficient of chips contraction. 64

List of Tables

Table 1: Summary of the Impact of titanium properties on machinability 22
Table 2: Different material properties [8] 23
Table 3: Chemical composition of Ti-6Al-4V.....29
Table 4: Cutting parameters during single point turning process 33
Table 5: Surface roughness measurement using uncoated inserts 35
Table 6: Ra measurement using single coated inserts 36
Table 7: Surface roughness measurement using multi coated inserts.....37
Table 8: Calculation of cutting time in minutes and seconds with respect to cutting speed.....37
Table 9: Optical microscopy of the chips microstructure at various cutting speeds and tool coatings by keeping feed and depth of cut constant, i.e. 0.16 mm/rev and 1 mm (20X magnification scale) 43
Table 10: Calculation of geometric parameters with respect to machining parameters for uncoated tool chips mechanism. 48
Table 11: Calculation of geometric parameters with respect to machining parameters for single-coated tool chips mechanism. 48
Table 12: Calculation of geometric parameters with respect to machining parameters for multi-coated tool chips mechanism. 49
Table 13: Calculation of response parameters with the help of geometric variables 50
Table 14: Design of experiments.....71
Table 15: Experimental details of turning test.....72
Table 16: Calculation of Material Removal Rate.....73
Table 17: Calculation of length of active tool engagement 74

1 CHAPTER 01

1.1 Introduction

In this chapter, a brief description of the project historical background including several methodologies. It includes project objectives, scopes of our thesis, problem statement of this project on prediction of surface roughness, surface integrity and chip characterization during CNC turning operation of Ti-6Al-4V.

1.1.1 Project Background:

In mythology, Titanium comes from the Greek word Titans, which means earth gods. Titanium is actually the ninth rich element (0.63% by mass) on the earth's crust. We have to find titanium in plants, the sun, stars, human body, and in seawater. The most important aspect of Ti is actually a high strength to weight ratio. In spite of the fact that aluminum is 60% less dense than titanium but when we examine the strength of titanium, it stacks up against the steel and titanium is 45% lighter. At room temperature, it becomes shiny, hard and strong.

High corrosion resistance is another incredible attribute of Ti. It provides excessive temperature resistance to alloys in addition to light-weight strength. The density and melting point of titanium are 4.5g/cm3, 1941K (1668^{o}C, 3034 ^{o}F). Titanium is utilized in joint substitution medical procedures due to the fact, metallic elements like titanium bonds properly with bones and is non-dangerous to completely different tissues.

The ultimate reliable application of titanium is in paints. When titanium bonded with oxygen, it becomes Titanium Oxide and this combination gives bright white color in paints. The compounds of titanium are majority violet in color. There are variety of fundamental and mechanical properties of Ti alloys. The pure industrial titanium has a elasticity range from 275 to

590 MPa, and this unique feature is controlled by using iron and oxygen constituents. The ratio of oxygen and iron substance is directly proportional to the quality and strength ratio (i.e. specifically for high quality and strength alloy Ti-15Mo-5Zr-3AI) [1].

Rapid Machining (HSM) is the foremost propelled accomplishment that had been created throughout the years. It has enabled the increase in efficiency, accuracy and quality of work pieces while at the same time decreasing costs and machining time (Schulz, H., 2003). Salomon's research demonstrated that there is a sheer scope of cutting rates where machining is impossible because of exorbitantly high temperatures. This is the main cause for which HSM can also be allude to as the cutting speeds beyond that range. In consistence with advance knowledge, a few analysts characterize high speed machining as machining whereby ordinary cutting speeds are surpassed by a factor of 5– 10 as shown in the figure.

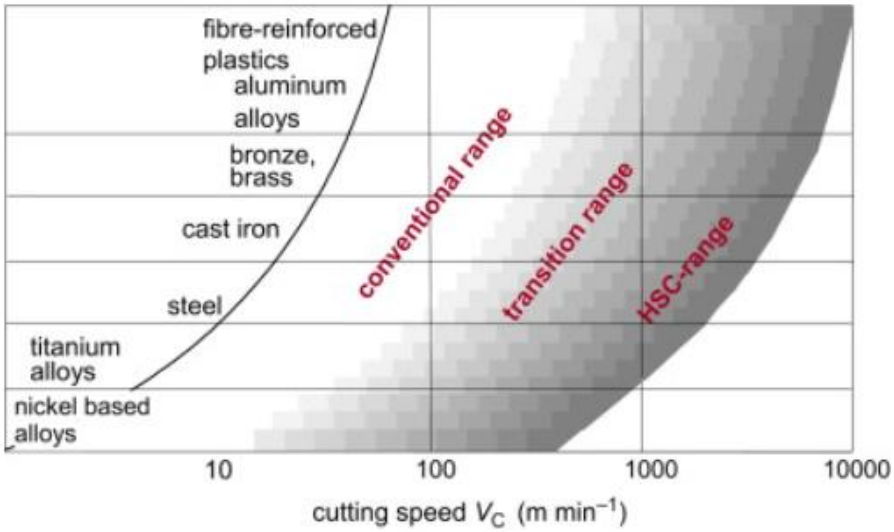

Figure 1: Area dependence on material/work piece [1]

1.1.2 Project Design:

The figure shown below represents the complete analytical procedure of my research. The design shows the methodology which I have adopted during my thesis.

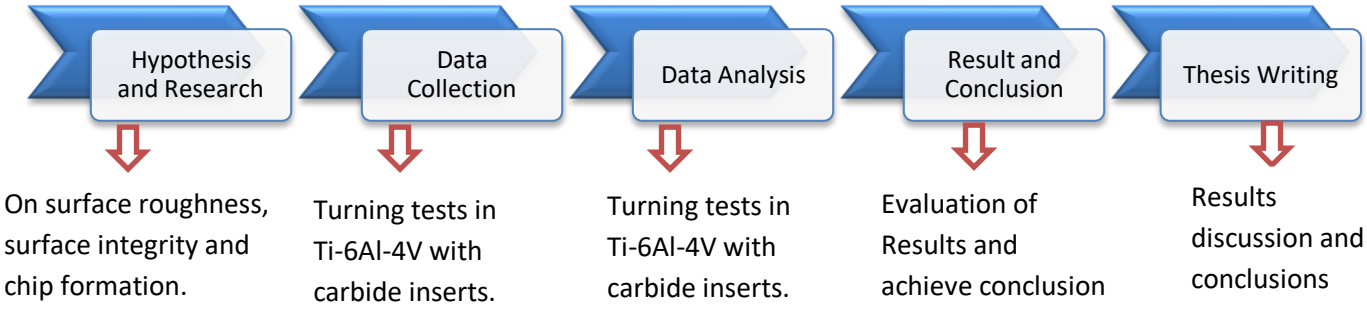

Figure 2: Project design

1.1.2.1 Problem Statement:

Titanium alloy grade 5 (Ti-6Al-4V) has less tool life and poor machinability relative to other materials. During the machining, huge amount of heat generated and absorbed in the material which is difficult to transfer. In general, tool deterioration needs to be controlled and diminished the cost of production and consequently increases tool life. Surface roughness is one of the essential financial aspect for enhancement of the life of cutting tool while machining. The factors that cause this problem includes which form of material to be machined, suitable machining parameters, i.e. feed, speed and depth of cut.

Another mechanism that affects the wear progression is chip formation, due to the fact that the interaction between cutting insert and chip generates crater and flank wear. By investigating and analyzing these two parameters we can conclude the geometry and morphology of the chips that are generated at the output. These are the major causes of my research.

1.1.2.2 Project Objective:

Surface roughness and surface finish analysis is the core objective of my research that varies with respect to different cutting conditions along with varying the tool coatings, as well as to study the chip geometry and shear deformation while machining of titanium alloy. A recently created topography was researched and compared against references at distinctive cutting

conditions. Chip geometry, adiabatic shear bands and chip characteristics were believed to provide information about the chip formation mechanism. The pathway of my research is schematically explained and represented as shown the figure below;

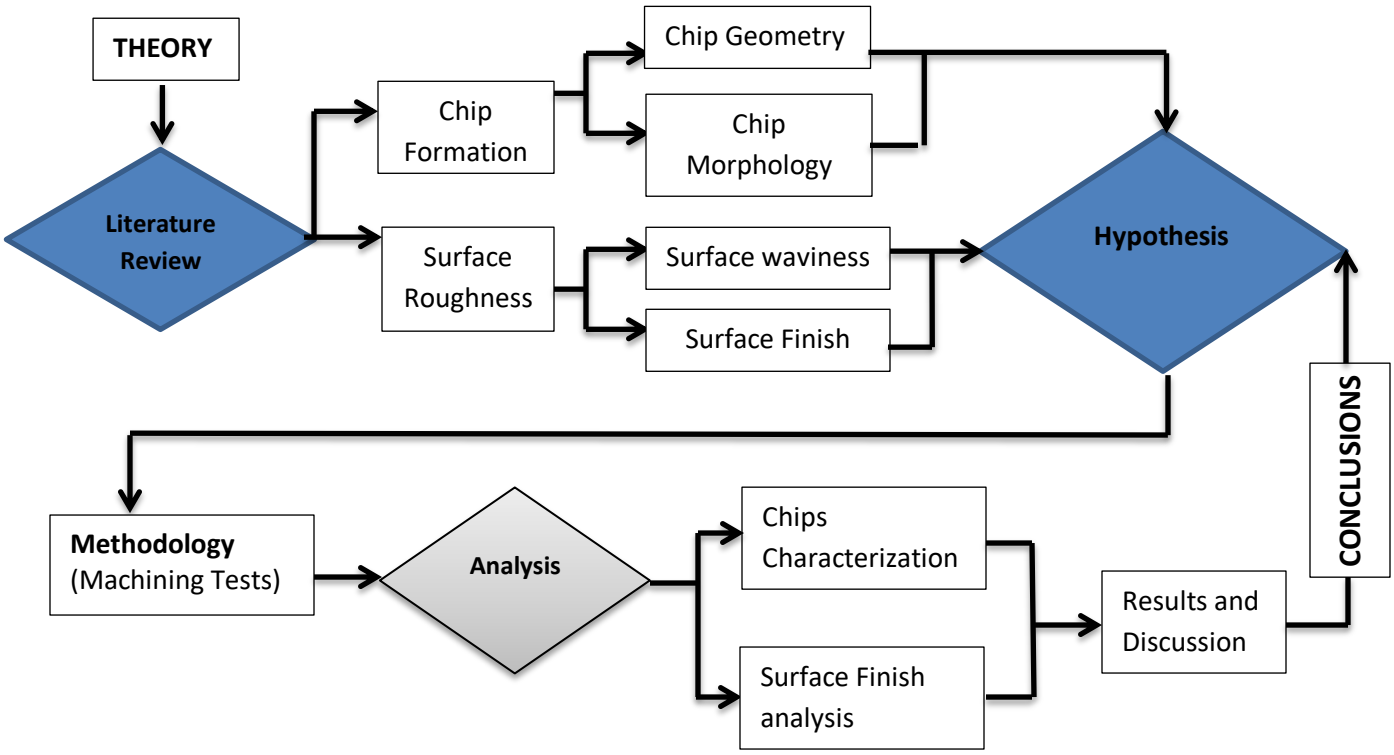

Figure 3: Schematic pathway and flow chart

1.1.3 Project scope:

As to accomplish the project objectives; the scope is listed as below:

- Assess and figure out the surface roughness by using TR 110 roughness meter in order to measure the surface waviness and surface finish of titanium alloy grade 5
- Evaluation and collection of machining chips of Ti-6Al-4V in order to analyze the chips characterization which includes mounting of chips at a certain temperature using Mounting machine, then grinding of the mounted chips using different sand papers and at the end polishing of the mounted chips using Grinder and Polisher machine.

- The selective parameters used for the single point CNC turning test of Ti6Al4V includes machining speed ranging from 50 to 150 m/min, Uncoated and PVD single coated and multi-coated inserts of Tungsten Carbide, by keeping Depth of cut, Length of Cut and Feed, constant at 1mm, 100mm and 0.16 mm/rev,.
- Analyze the surface roughness results and chip characterization by using Optical Microscopy and measure the chips morphology and geometrical parameters in ImageJ software.

2 CHAPTER 02

2.1 Literature review:

2.1.1 Impacts on machinability of titanium properties

The poor thermal conduction exhibits poor machinability of titanium alloys because of avoiding heat transfer into the work piece, extreme reactivity, low versatility and elastic modulus, high hardness at raising the temperature by increasing the cutting speed. These factors have an intense impact upon the tool life and tool deteriorates more.

Table 1: Summary of the Impact of titanium properties on machinability

Property	Description	Reference
Thermal Conductivity	Poor thermal conductivity causes the accumulation of heat at the cutting edge, thus reduces his life of cutting tool.	[2]
Elastic Modulus	Low elastic modulus creates chattering of the work-piece which results poor machinability.	[2, 3]
Strength and Hardness	Due to the extreme hardness and strength leads to enhancement of cutting forces, thus causes deformation of the cutting inserts during machining.	[4]
Work Hardening	This property avoids of making build up edges on the tool tip. Due to high heat accumulation at the tool-chip interface results increases in shear angle and bearing load per unit area. This may result sudden breakdown of the tool due to high heat generation.	[5-7]

Chemical Reactivity	During the machining of titanium alloys, it reacts with different gases to form hydrides, nitrides and oxides. These formations disturb the life of cutting tools, reduces the fatigue strength and significantly increases the tool wear.	[5, 6]

In order to enhance efficiency and tool life, High Speed Machining (HSM) is effective for producing high quality surfaces, without burr edges [8]. During high speed machining, the thermal impact reduces and huge amount of the heat radiation is consumed by the machining chips, tool deteriorates less, thus increase the life of the cutting inserts .

The machining method we followed is dry machining because of many reasons such as tungsten carbide tools, ceramics, titanium supports dry machining. Secondly, coated tools assist dry machining because coating helps to reduce friction and minimize the cause of heat propagation and it also reduces the cost of cutting fluids during machining. HSM has such a large number of favorable circumstances, it is usually applied in the aeronautics department, the automotive industry, and manufacturing industries for machine devices, gear, and tooling utilized in the making of household apparatuses, optics, and so forth [8].

In normal HSM applications, huge deformation and shearing occur on the shear plane side, while machining. Likely, due to workpiece flexibility, chip formation have been classified into following types: constant and shear-restricted. Regularly the consistent chips have significant quality, and geometry of chip is the main issue going up against researchers [8].

Table 2: Different material properties [8]

Material	Thermal Conductivity W m^{-1} K	Specific heat capacity J kg^{-1} C	Tensile strength M Pa

Aluminum 7075-O	173	960	96.5
AISI 4340 Steel	44.5	475	786
Ti6Al4V	6.7	526.3	1100
WC-Co (6-10%)	60-80	200-400	1440

Surface roughness analysis is a critical framework, thus impact the work piece quality. The mechanical device's efficiency is a vital Desired value of surface roughness of a product is generally defined to achieve the required fatigue strength, corrosion resistance, precision fits, tri-biological and aesthetic requirements. In this way, estimating and describing the surface finish has been considered as the translator of machining execution and performance [9].

2.1.2 Previous research on Surface Roughness and Surface integrity:

Prediction model of surface roughness with respect to processing parameters has been broadly discussed in the literature by using response surface methodolgy [9]. This it showed that the feed and spindle speed creates greater effect on the surface roughness (Ra), while the other parameter i.e. depth of cut played negligible effect. The consequences of radial rake angle associated with feed and cutting speed gave huge impact on Ra by AzlanMohd Zain et al.[10]. He concluded on his research that by increasing the values of radial rake angle, spindle speed and decreasing the value of feed should reducing the value of Ra. Another scholar Selvakumar et al.[11] worked on the cermet inserts and concluded that feed and inserts types had greater impact on the response surface.Ramesh et al.[12] worked on turning of Ti6Al4V and analysed that individual parameter which plays huge impact on roughness value is basically the feed rate. Chauhan[13] evaluated the consequences of processing parameters, entering angle and tangential forces, while turning of titanium alloy. Ezugwu and Wang[14] , Ribeiro et al.[15], Rahman et al.[8], Yang and Liu.[16] and Ezugwu.[17] highlighted the core issues and analyzed that what are the factors that effects

on the tool deterioration and failure. Ribeiro et al.[15] executed experiments with uncoated tungsten carbide inserts and analysed that by changing the processing parameters, what is the impact on the tool deterioration during turning. In the machining of titanium alloys, a lot of heat accumulation at the cutting face and difficult to transfer heat, just because of low thermal conductivity. In the literature, lubricants were used in order to compensate and reduce heat gereration and increase the life of cutting inserts and minimize the Ra and tool wear value.

The factors that really effects to increase the surface roughness values are; type of material and tool used, machining parameters to be selected, Tool nose radius, Length and diameters of the selected material, Chips morphology and geometry, fluctuations in the cutting forces, Chattering, and heat generation at the cutting interface of the inserts [18].

2.1.3 Previous Research on Chips Morphology and Characteristics:

Chips characterization and morphology is another distinctive phenomenon in order to analyze the chip geometry. Many authors worked about the morphology of the chips. The question arises, why the chip geometry changes and what are the factors which are being effected for changing the structure. Calamaz et al. (2008) told that the selection of processing parameters for machining and surface roughness and integrity plays a dominant role that which type of chips emitted.[19] Mainly, chips are classified as continuous, discontinuous, continuous chips with build up edge and segmented which is also called serrated chips.

For shifting the categorical behavior, type of material used, rake angle and machining parameters considered to be the main cause. As in case of continuous chips emission, the material should be ductile, rake angle must be high, cutting speed should be high or medium and depth of cut (DOC) must be small. For discontinuous chips, the material must be hard whether it would be

ductile or brittle, rake face should be medium, depth of cut must be high, and lower cutting speed. Continuous chips with BUE includes ductile material, rake face would be low or medium and medium spindle speed and DOC. Segmented chips are also called non-homogeneous chips, which exhibits low thermal conductivity, strength metallic behavior and it must have different shear strains and primary, secondary shear zones.

At the tool chip interface, various zones are going to be emitted as shown in the figure below and temperature is high due to concentration of heat on distinctive zones. Due to heat accumulation, zones would be made and its shape is sawtooth like behavior with semi-conductive or segmented chips. The materials which has low thermal conductivity similar to that of my work-piece creates tool deterioration to be very high [20] because of certain circumstances;

- Creates high shear zones due to extreme heat generation at the cutting face.
- As due to the high reactivity of titanium, material react with the tool interface and different sort of molecules adhere create build-up-edge (BUE), thus results initiation of tool deterioration and reduces life of cutting inserts.

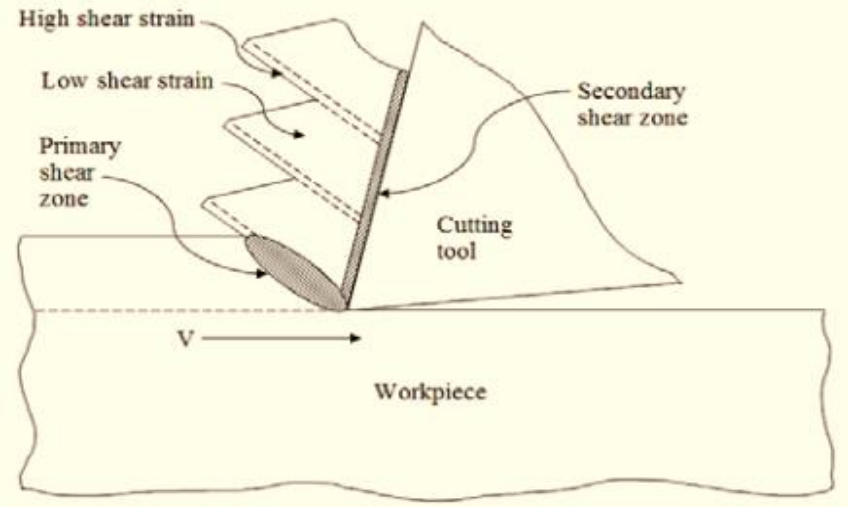

Figure 4: Different zones of chips for single point turning [21]

2.1.3.1 Chips Formation

Chip development strongly impacts on the cutting forces, power, life of cutting inserts, tool deterioration and value of Ra. In this manner, it is vital to comprehend the cutting conditions that outcome in chips that are anything but difficult to deal with and limit the negative impacts on the cutting inserts and work piece surface. Different sort of shear zones and adiabetic shear bands were formed and it is the most important aspect of investigating these shear zones and band width [22]. On the other hands, chip geometry is another unique feature for analyzing the of morphology of cutting chips.

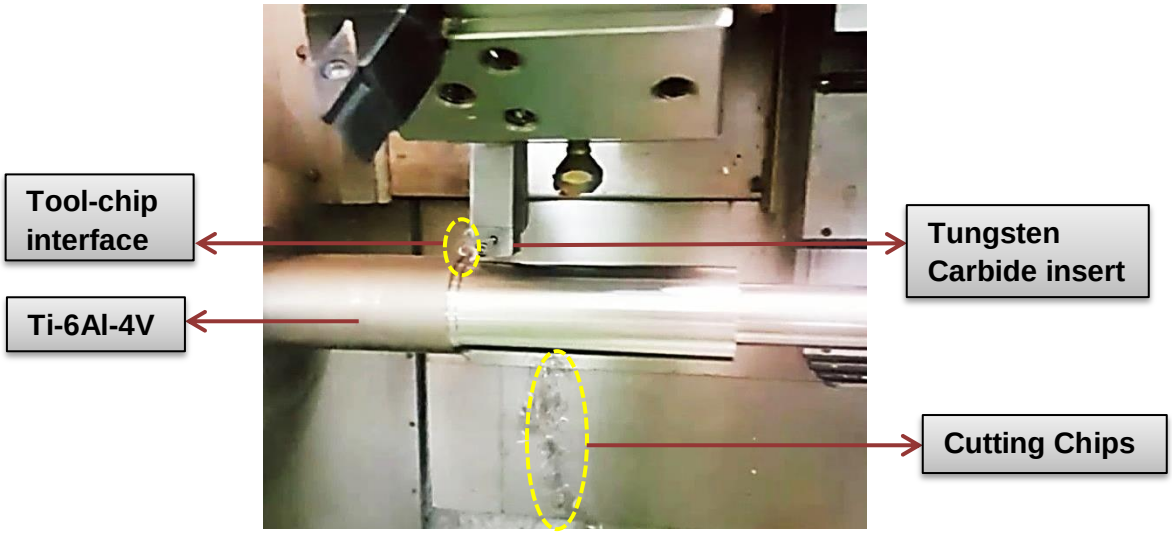

Figure 5: Single point CNC Turning

While machining, chip adhesion on the tool tip plays a huge impact on the tool, thus results tool deteriorates more. Due to high heat generation, a spark is produced and welds the chip pieces on the tooltip, making BUE at the cutting interface. Chip thickness with feed-rate also effect on the roughness value. Optimal finished surface and improved chip thickness is achieved by decreasing the rate of feed and increases the spindle speed. Thickness of cutting chips and surface quality affected by decreasing the value of feed and this will give high value of surface roughness [23].

3 CHAPTER 03

3.1 Methodology:

In this chapter, there is a complete summary of testing methodology and analysis of surface roughness and chip characterization.

3.1.1 CNC Turning Test:

A 45x395 mm dimension of the workpiece material i.e Ti-6Al-4V alloy was used to perform experiments. Ti-6Al-4V was tested on the machine named Portalbe XRF XL3t GOLD + Carbon Analyzer Spectrophotometer (Optical Emission Spectrometer) in order to find the material chemical and elemental composition. The Brinell Hardening test was performed to measure and check the indentation of the material i.e. 103 HRB.

Figure 6: ML-300 CNC Lathe machine

The Table 3 presented below defines the chemical composition of Ti6Al4V. Experimentation would take place on CNC lathe machine Model ML-300 with FANUC 0i-TC controller. The

machine specifications are presented below. Tungsten Carbide Inserts **CCMW09T304H13A** were used with the help of tool holders to perform turning operations.

3.1.2 CNC Lathe machine specification.

- Diameter X Length: ⌀300 x 600mm
- Max travel range of Z/X axis: 600/240 mm

3.1.2.1 Standard Accessories:

- FANUC 0i-TC Controller
- Spindle Speed: 3500 RPM
- 10- Tool Hydraulic Turret
- Manual Body Hydraulic tailstocks
- MT No. 4 tailstock Quill, Coolent system
- Chip Conveyor + Chip Bucket
- Automatic Lubrication System, work lamp

Table 3: Chemical composition of Ti-6Al-4V

Elements	Min (>=) %	Max (<=) %	Calculated %
Fe		0.4	**0.2**
V	3.5	4.5	**4.3**
Al	5.5	6.75	**5.7**
O	-	0.2	**0.16**
C	-	0.08	**0.07**
N	-	0.05	**0.045**
Ti	-	-	**89.81**

3.1.3 Operational Setup:

The experimental configuration for the turning operation is shown in the figure; where $\mathbf{v_c}$, $\mathbf{f_n}$, $\mathbf{a_p}$ are the cutting speed, feed rate and depth of cut.

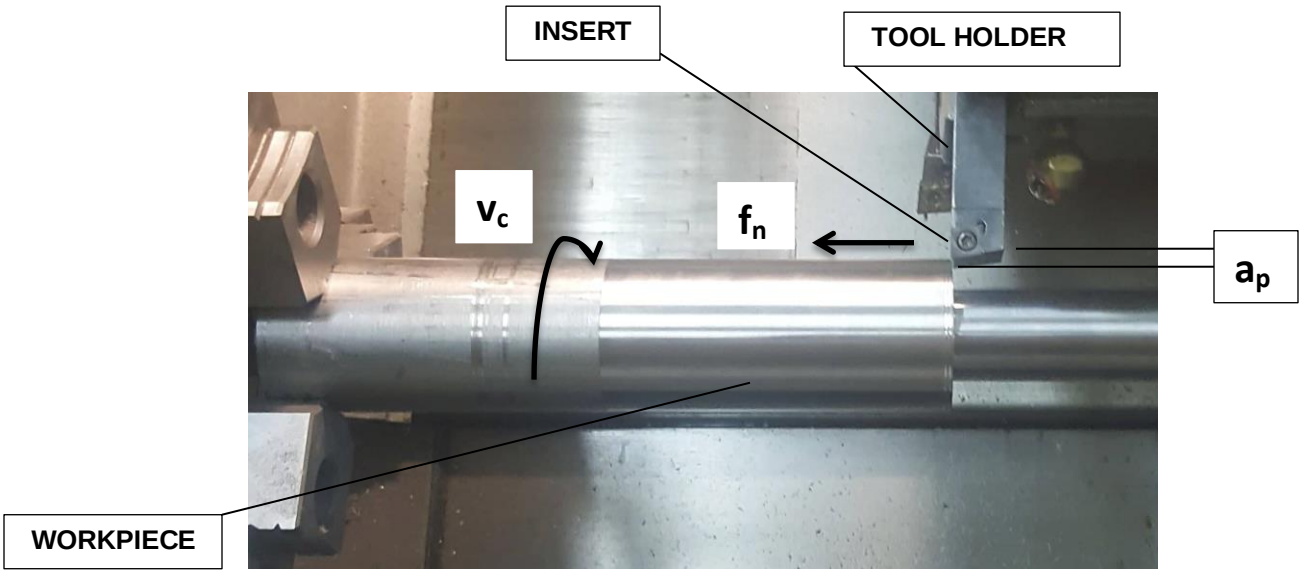

Figure 7: Operational Experiment setup of CNC turning machine, V_c = Cutting speed, f_n = Feed rate, a_p = Depth of cut

3.1.4 Cutting Tools:

The cutting inserts used for single point CNC turning of titanium alloy had a CCMW09T304H13A geometry. Dry machining tests were performed by using tungsten carbide inserts CCMW09T304H13A T-MAX U T-MAX CLAMPED TYPE AND T-MAX S TU.

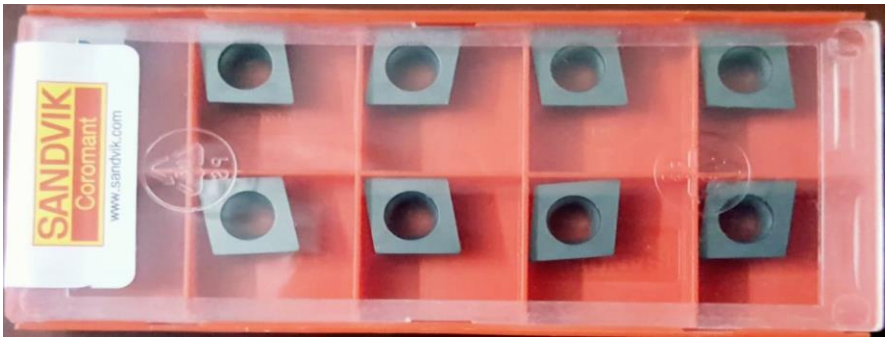

Figure 8: Tungsten Carbide SANDVIK inserts

These inserts were purchased from G.E Tools Limited, United Kingdom. Three types of inserts coating were used for experimentation namely, "Uncoated, Single-coated and Multi-coated". From the main catalogue (Cutting tools from Sandvik Coromant), The clearance angle is 7^{o}, Entering angle is 95^{o} with an insert thickness (s) of 3.97, Tolerance on Class 's' is ± 0.13 and the nose radius is 0.4 mm. The main aim to use a TiAlN coating is to have a high abrasive wear coefficient as compared to other types of coatings.

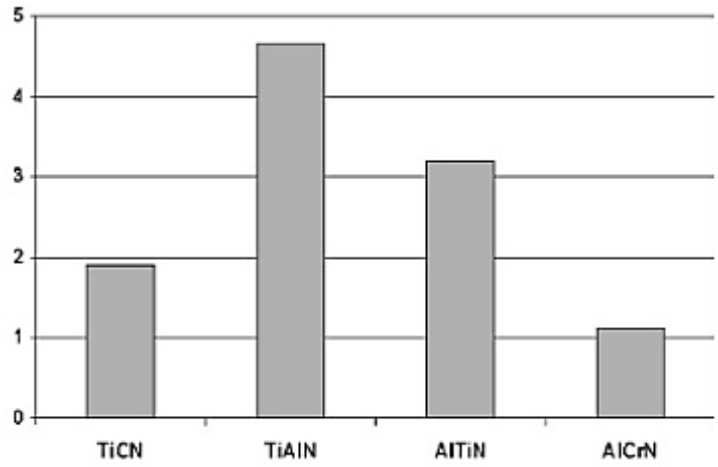

Figure 9: Abrasive wear coefficient of different coatings [24]

As, the literature clearly shows that TiAlN coating has the highest value of abrasive wear resistance which is approximately 4.8 as compared to AlTiN coating which is approximately 3.2. The least possible value of abrasion resistance is at 1.2 of AlCrN coated tools. In multi-layer coating, that's the reason to first deposit the TiAlN layer, then deposit the second layer of CrAlN.

3.1.4.1 Tool Coatings Specifications:

As by increasing the life of cutting inserts, reduction in tool deterioration and observe the trend of roughness value is the core objective to perform coating.

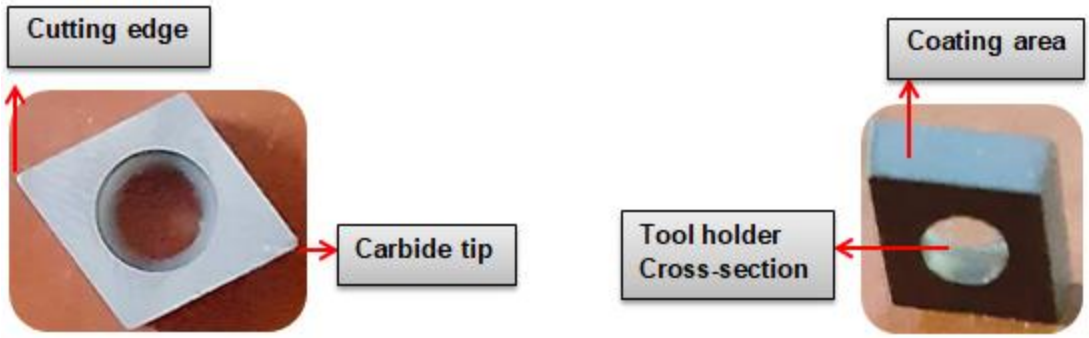

Figure 10: Tungsten Carbide Schematic view

Detailed specifications of coatings to be performed on inserts are as follows:

- PVD coating consists of a single layer of Titanium Aluminum Nitride Coating (TiAlN):
- PVD coating consists of multilayer of Titanium Aluminum Nitride + Chromium Aluminum Nitride (TiAlN + CrAlN) coating:

In multi-layer coating TiAlN is to be deposited on the inner side while CrAlN is to be placed on the other side because of thermal conductivity.

- Coating Thickness in single layer coating: 1.5 microns
- Coating thickness in multi-layer coating: 1.5 microns each

A total of 27 experiments was performed on CNC Lathe Machine. The design of experiments is presented in the Appendix A1.

3.1.5 Cutting Parameters:

Nine cutting speeds between 50 m/min and 150 m/min were investigated. Depth of cut, Length of cut and Cutting feed were kept constant at 1.00 mm, 100 mm and 0.16 mm/rev, respectively. I have selected these parameters from the wear rate map;

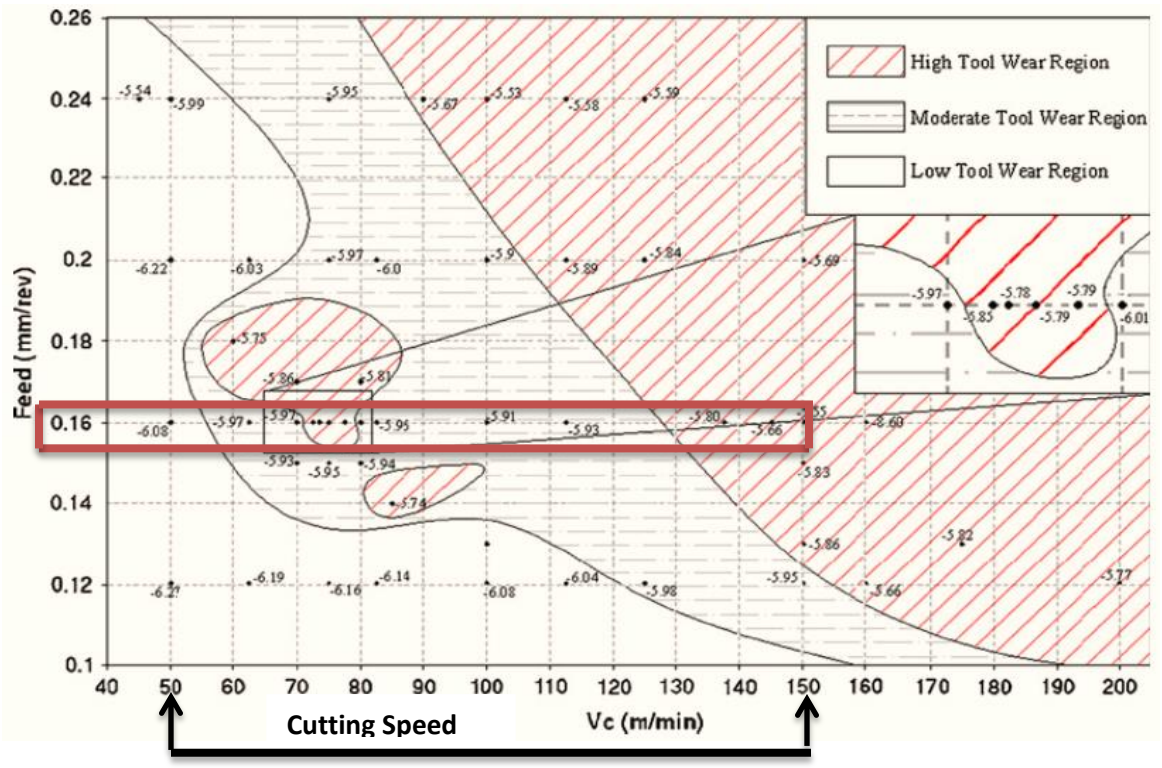

Figure 11: Wear map for turning test of Ti-6Al-4V [25].

Different types of regions is completely highlighted and explained in the wear rate map. Each is distinguished by different types of hatching lines.

Table 4: Cutting parameters during single point turning process

Cutting Speed (m/min)	50	55	60	62.5	65	70	100	130	150
Cutting Feed (mm/rev)	0.16	0.16	0.16	0.16	0.16	0.16	0.16	0.16	0.16
Depth of Cut (mm)	1	1	1	1	1	1	1	1	1
Length of Cut (mm)	100	100	100	100	100	100	100	100	100

3.2 Surface Roughness (Ra) Analysis

Firstly, I have performed 9 experiments by using uncoated inserts of tungsten carbide. As, I have already mentioned the cutting parameters in table 4. For the completion of every run, I have

collected the chips in the zipper bags and measured the surface roughness (Ra) and surface finish. For the measurement of Ra value of titanium alloy, the Roughness Meter of Model No " TR110 " was used.

Figure 12: Surface Roughness Meter

3.2.1 Surface Roughness Description:

- Stylus mark
- Switch of sensor stylus protective sheath
- Crust of main body
- Left key
- Middle key
- Right key
- LCD
- Start key
- Charging socket
- Back cover lock

- Label

Figure 13: Schematic figure of Surface Roughness meter

3.2.2 Type A:

The factors which influence on the Ra includes tool and work piece vibration during machining, nose radius of the cutting inserts, tool deterioration, type of material and inserts used and the chip geometrical parameters, shear deformation zones, heat generation and accumulation of chips. The measurement of type A uncoated inserts average roughness values (Ra) in microns was shown in the table;

Table 5: Surface roughness measurement using uncoated inserts

Feed (mm/rev)	Speed "V_c" (m/min)	Depth of cut (mm)	Linear Length of cut (mm)	Avg. Surface Roughness R_a (microns)
0.16	50	1	100	**1.75**
0.16	55	1	100	**1.45**
0.16	60	1	100	**1.79**
0.16	62.5	1	100	**1.50**
0.16	65	1	100	**1.58**
0.16	70	1	100	**1.55**

0.16	100	1	100	**1.48**
0.16	130	1	100	**1.27**
0.16	150	1	100	**1.00**

3.2.3 Type B:

For the type B which is single coated inserts of TiAlN coating, the measured average roughness values (Ra) in microns were presented;

Table 6: Ra measurement using single coated inserts

Feed (mm/rev)	Speed "V" (m/min)	Depth of cut (mm)	Linear Length of cut (mm)	Avg. Surface Roughness R_a (microns)
0.16	50	1	100	**1.68**
0.16	55	1	100	**1.77**
0.16	60	1	100	**1.56**
0.16	62.5	1	100	**1.96**
0.16	65	1	100	**1.55**
0.16	70	1	100	**1.79**
0.16	100	1	100	**1.48**
0.16	130	1	100	**1.24**
0.16	150	1	100	**1.29**

3.2.4 Type C:

For the type C which is multi coated inserts of TiAlN + CrAlN coating, the measured average roughness values (Ra) in microns were given in the below table;

Table 7: Surface roughness measurement using multi coated inserts

Feed (mm/rev)	Speed "V_c" (m/min)	Depth of cut (mm)	Linear Length of cut (mm)	Avg.Surface Roughness R_a (microns)
0.16	50	1	100	**1.82**
0.16	55	1	100	**1.47**
0.16	60	1	100	**1.91**
0.16	62.5	1	100	**1.83**
0.16	65	1	100	**1.46**
0.16	70	1	100	**1.78**
0.16	100	1	100	**1.70**
0.16	130	1	100	**1.64**
0.16	150	1	100	**1.27**

3.3 Length of active tool engagement analysis:

As it is clearly defined, namely that how much time, the tool, i.e insert was engaged with the workpiece i.e. grade 5 titanium alloy to remove the material. It is also called cutting time. For the cutting speeds of 50 to 150 m/min, the value of cutting time, which is length of active tool engagement decreases while increasing the cutting speed as shown in the table below;

Table 8: Calculation of cutting time in minutes and seconds with respect to cutting speed

Sr No	Feed mm/rev	Speed "V_c" m/min	Depth of cut mm	Tc (sec)	Tc (min)
1	0.16	50	1	**106.03**	**1.77**
2	0.16	55	1	**92.11**	**1.54**
3	0.16	60	1	**80.50**	**1.34**

4	0.16	62.5	1	**73.51**	**1.23**
5	0.16	65	1	**67.06**	**1.12**
6	0.16	70	1	**58.90**	**0.98**
7	0.16	100	1	**38.88**	**0.65**
8	0.16	130	1	**28.09**	**0.47**
9	0.16	150	1	**22.78**	**0.38**

3.4 Chip formation analysis:

During the single point turning, the material was removed in the form of machining chips, which was collected in the zipper bags for examination. The type of chips is generally based on the geometry of cutting tool, type of inserts, selection of machining parameters and work piece selection. As during my experimentation, I have observed that for high machining parameters, i.e. for high cutting speeds, the burning of chips inaugurate at the cutting interface. Secondly, for low cutting speeds, lesser tool deterioration would occur and life of tool will increase for selecting these parameters.

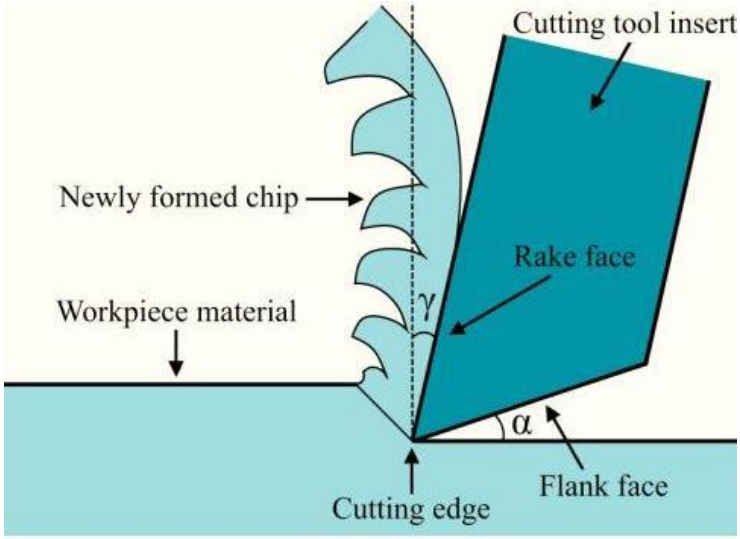

Figure 14: Chips Morphology at the Insert - Material interface

3.4.1 Sample Preparation:

For analyzing the morphology of chips, first we need to make a mold in which piece of cutting chips were placed. For making the mold, Mounting mechanism is the most appropriate method in order to investigate the chip characteristics. Chip sample would place on the vertical placement bar of "Hydropress Mounting Machine" which is also called Automatic Mounting Machine. Shower the specific amount of Conductive mount Graphite powder (containing only black graphite) over the sample and covered the mounting press with a plunger. Set the temperature T (S_u) of 190^{o}C, wait for 20 minutes to achieve the mounted sample. After completion of cycle, machine beep would be heard, which is basically the indication to collect your sample specimen. Repeat this mechanism again and again for all the chip samples which is to be analyzed.

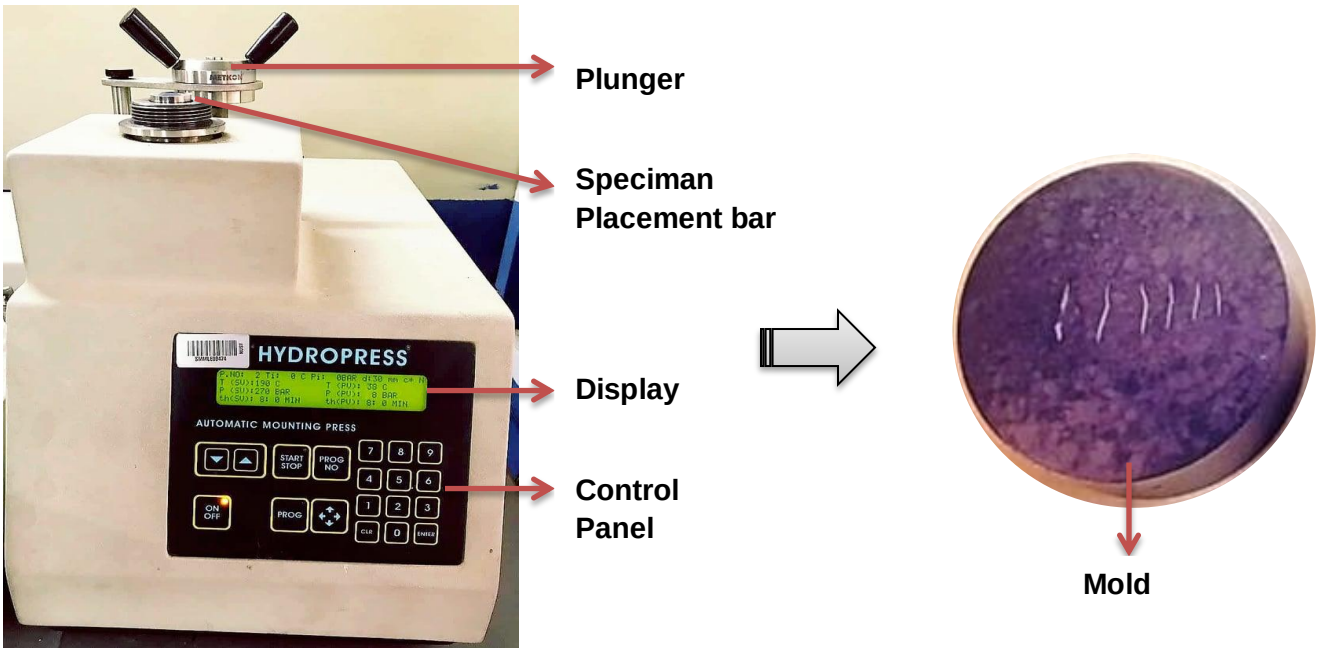

Figure 15: Hydro press Mounting Machine and achieved chips Mold

Further, mounted mold samples were then grinded by using different abrasive grinding papers, i.e. Silicon Carbide (water proof) grinding papers. The machine used for grinding and polishing of samples was "Metkon GRIPO 2V Grinder Polisher Machine". First, the molds were grinded

by using 800 silicon carbide grinding papers to trim mold surface. Then shifted to 1200, 2000, 2400 and at the end when the surface was nearly finished (smooth), 4000 abrasive grinding papers would be used to trim the surface at that level, when the microstructure of the mold surface would be clearly highlighted. When shifting the mold surface from one silicon carbide grinding paper to another or preparation from grinding towards polishing, the mold surface must be washed with a detergent, water and ethanol.

Figure 16: Metkon GRIPO 2V Grinder, Polisher Machine

At the end, polishing pads were used using different grades of slurry powder. Extra fine and smooth surface was the main objective. First, the mold surface was polished with a polishing pad using 6µm slurry powder. After completion of this step, wash the surface with detergent, water and ethanol. Then, polished the surface with 3µm and 1µm slurry powder to make the surface extra fine and shine.

Ti-6Al-4V Uncoated Chips cross sectional area

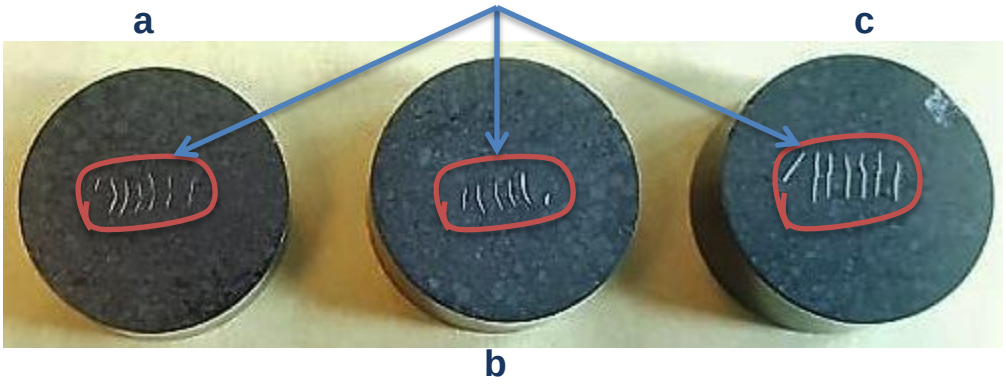

Figure 17: Mounted graphite pellets with uncoated cross sectional of chips:

a f=0.16 mm/rev, V_c=50m/min; b f=0.16 mm/rev, V_c=70m/min: c f=0.16 mm/rev, V_c=150m/min

As the alloys of titanium have high ductility because of this property, Ti has easily scratched during polishing of mold surface. This was the main reason, to use different grades of slurry material and to polish the mold surface step by step. Samples were then washed and cleaned at every stage during grinding and polishing of mold surface. Figurative images of uncoated, single and multi-coated chips molded cross-sectional surfaces at various selective parameters shown in the figures;

Ti-6Al-4V Single coated Chips cross sectional area

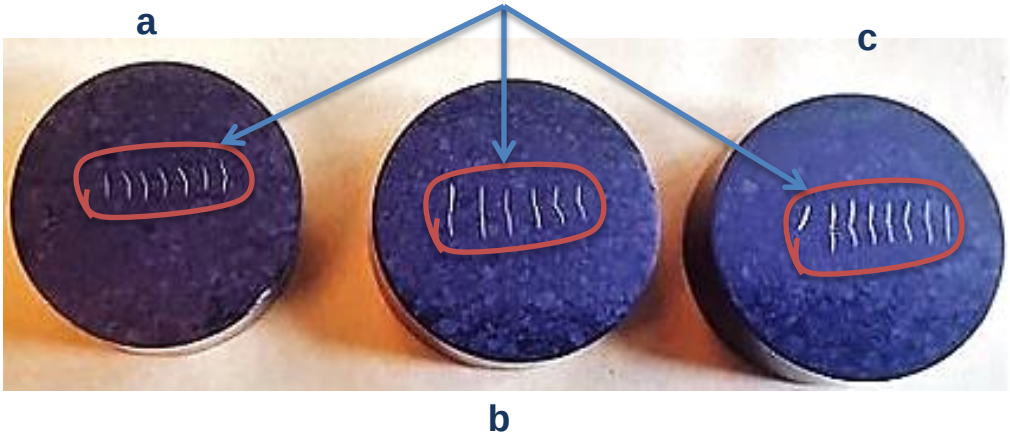

Figure 18: Mounted graphite pellets with single-coated cross sectional of chips:

a f=0.16 mm/rev, V_c=50m/min; b f=0.16 mm/rev, V_c=70m/min: c f=0.16 mm/rev, V_c=150m/min

Ti-6Al-4V Multi-coated Chips cross sectional area

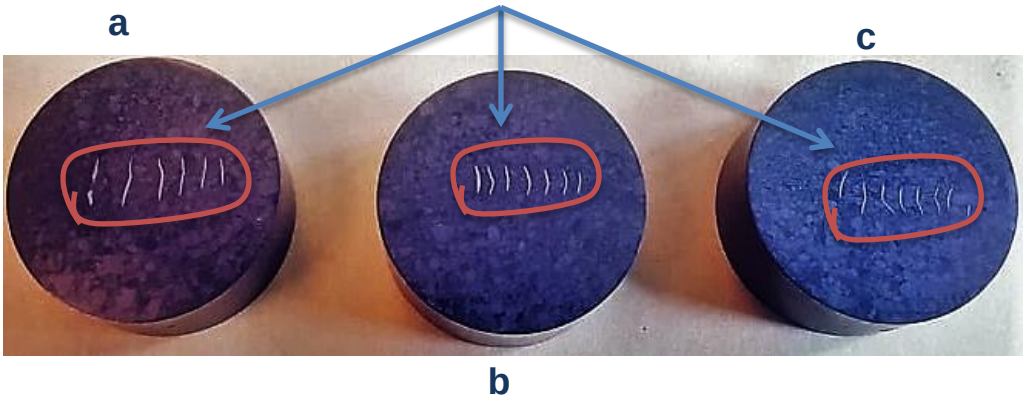

Figure 19: Mounted graphite pellets with multi-coated cross sectional of chips:

a f=0.16 mm/rev, V_c=50m/min; b f=0.16 mm/rev, V_c=70m/min: c f=0.16 mm/rev, V_c=150m/min

3.5 Chip Characterization:

During the completion of every experimented, Titanium alloy chips were collected and placed inside the zipper bags for the uncoated, PVD single coated and multi-coated samples. Optical microscopy was performed for analyzing the chip geometry, chips morphology and chip mechanism.

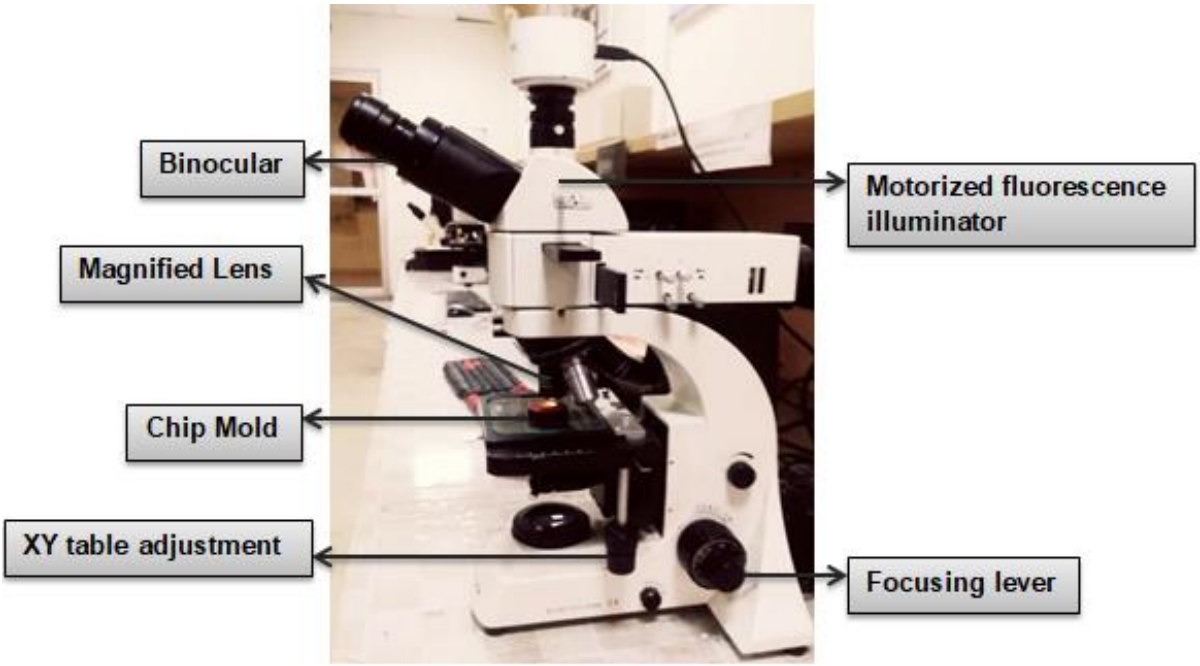

Figure 20: Optical Microscopy Analysis

During the machining of workpiece, inserts were deteriorated on the crater and flank side. This crater and flank wear cause and affects the chips morphology and mechanism, thus terminates the change of chip size, shape and geometric parameters. Due to this reason, chips were studied under the optical microscope namely OPTIKA 600 in order to measure the fluctuation in shapes, size and identify adiabatic shear bands and cracking area.

After grinding and polishing of chips, samples were cleaned with water, detergent, rinsed with ethanol and at the end dried at every stage before placing under the optical microscope. Following are the reasons, why the chip geometry varies with respect to processing parameters;

- Crater wear of tool
- Flank wear of tool
- Periodic variation of cutting forces
- Vibration of tool (insert) during machining
- Surface integrity
- Material selection

As it is clearly demonstrated in the figure that the deformed chip thickness, chip segmentation, shear bands, saw tooth peaks, continuous and separated portions and chip geometry changes by varying the processing parameters and type of coating.

Table 9: Optical microscopy of the chips microstructure at various cutting speeds and tool coatings by keeping feed and depth of cut constant, i.e. 0.16 mm/rev and 1 mm (20X magnification scale)

V_c m/min	UNCOATED CHIPS	SINGLE COATED CHIPS	MULTI COATED CHIPS

50	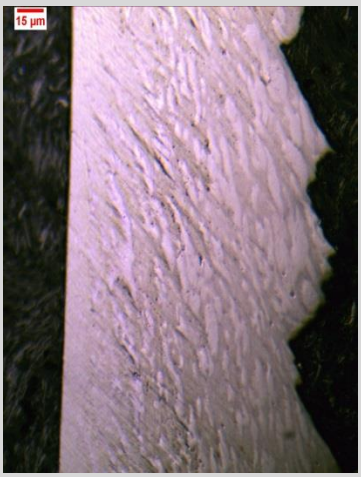		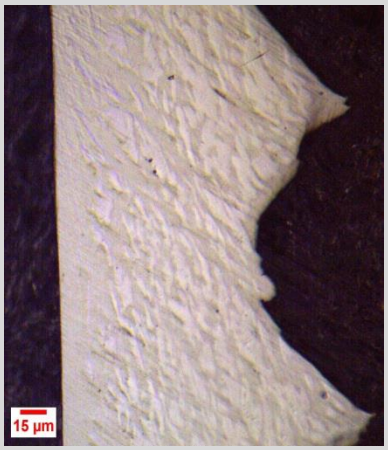
70		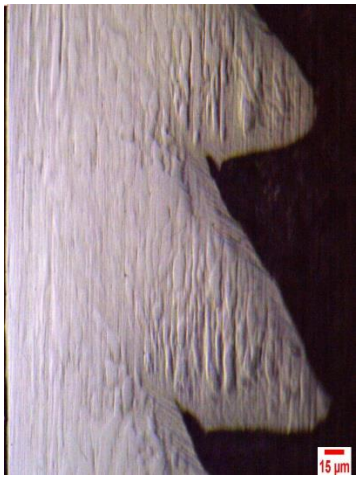	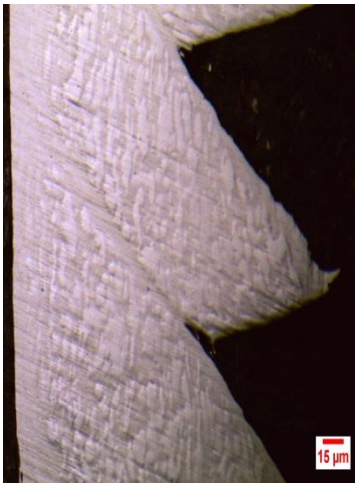
150	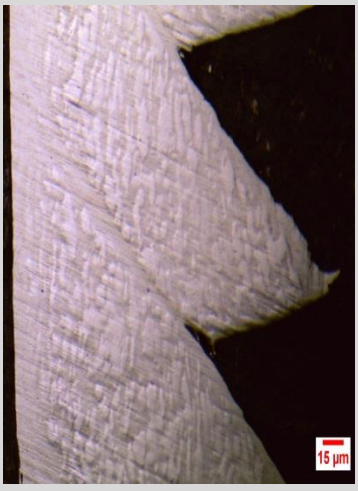		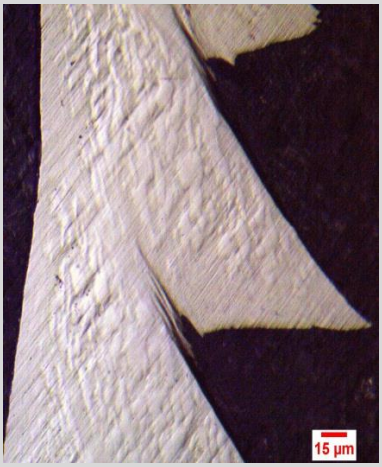

These chips segmentation has “saw tooth” like structure with chip waviness to be smoother on the outer surface and all the segmented chips have classified into two portions. One is the separated portion (chip waviness) and another one is continuous portion. I have analyzed and observed a total of 9 samples, 3 of each type of coating and the magnification scale was set and calibrated at 20X and the purpose to set this scale was to analyze and clearly visualize the chip morphology, microstructure and geometrical parameters of the chips.

3.6 Optical Microscopy: Chip Geometry and Morphology

For analysis, an INFINIFIX Optical system, Binocular microscope is used. The Vision camera was used to image the microstructure of chips morphology, and geometric parameters with the software Optika Vision lite. Geometric parameters include the height of the peak (H_P), height of the valley (H_v), complimentary angle (θ'), tooth pitch (P_c), shear angle (Φ), segment ratio (G_s), equivalent deformed chip thickness (T_c), chip segmentation frequency (F_{cs}), chip thickness ratio (r), chip reduction coefficient (1/r).

Geometrical features of chips gave information about the residual stresses, surface quality, consumption of energy, tool life and the machining effects. For uncoated, single coated and multi-coated chips, molds were placed under the 10X, 20X magnification lens and adjust the longitudinal and transverse knob so that to achieve clear and precise images in order to easily analyze the microstructure, cracking portion, adiabatic shear bands, chips morphology and characterization.

Figure 21: Optical Microscope OPTIKA 600 connected with PC

Once the images were captured, then import the images into OPTIKA Calibration software, i.e. OPTIKA view, to achieve calibrated images and calibration scale. The purpose of calibration is to measure the geometry of chips morphology on ImageJ software 1.38version. Calibrated scale would help to measure the geometrical parameters accurately.

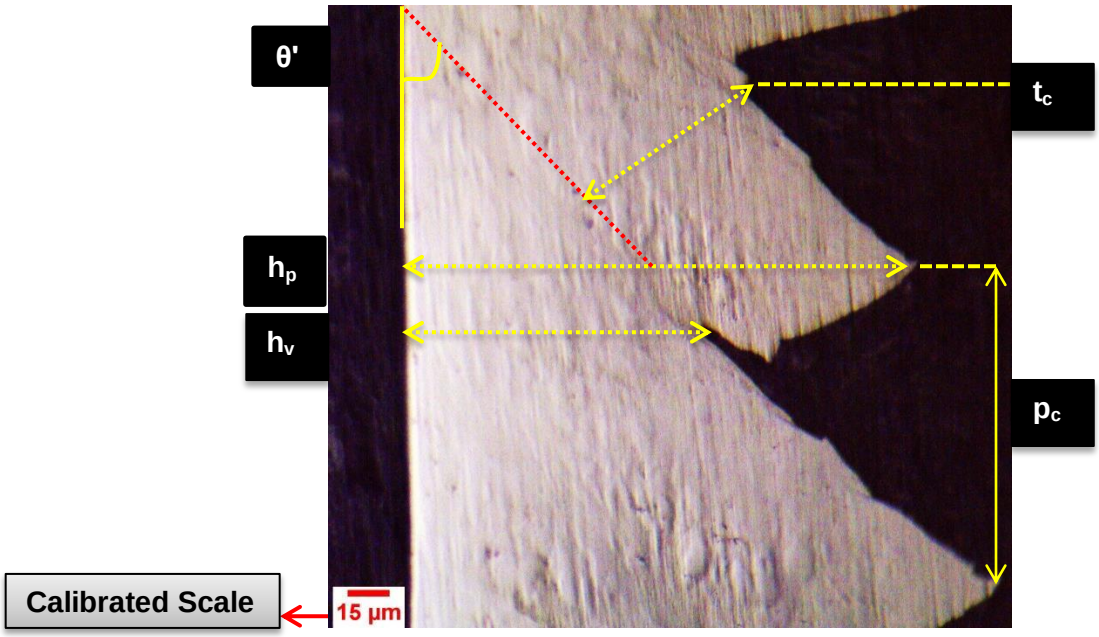

Figure 22: Serrated section of chip

The representation of serrated chip morphology is shown in the above figure which illustrates the geometric parameters and chip characteristics, i.e. $\mathbf{h_p}$ is basically the peak height, $\mathbf{h_v}$ denotes

height of valley, $\mathbf{p_c}$ is the tooth pitch or in generic we called it peak to peak distance, $\mathbf{t_c}$ expresses the equivalent deformed chip thickness and **θ'** denotes the complementary angle of the given chip morphology.

On the basis of physical properties, Ti alloys produce serrated chips and shear deformation was not uniform thus, make saw-tool like structure. Two types of zones were made, primary and secondary shear zones because of the extreme amount of heat generation. Just between the tool-chip interface, the primary shear zone was formed and the secondary shear zone was formed at tool-chip contact side. The figure below clearly shows, secondary shear zone, adiabatic shear bands, crack initiation on the chip cross-section.

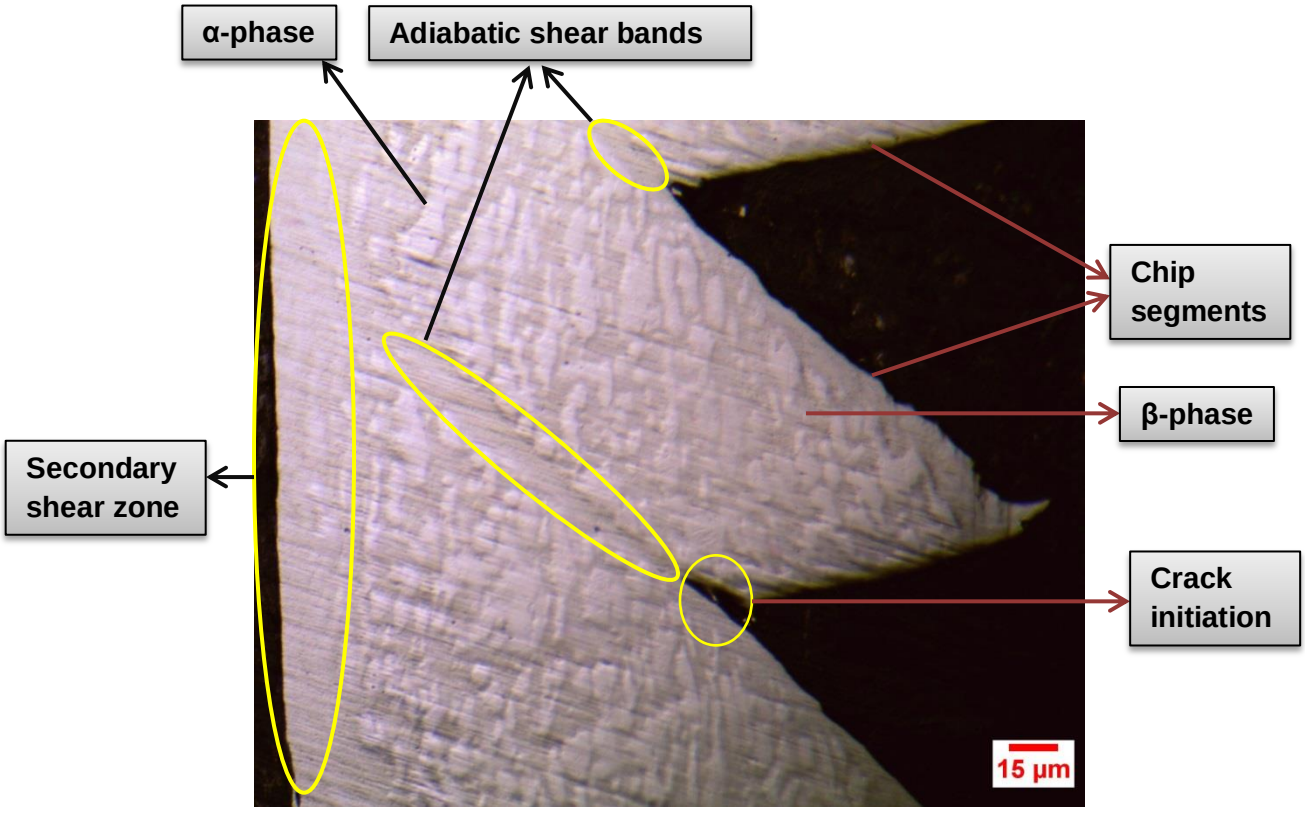

Figure 23: Adiabatic shear bands, Crack initiation, Secondary shear zone, chip segments localization in the given chip morphology

These segmented were formed just because of high heat generation and poor thermal conductivity. The irregular patches or zones appeared in the chip cross section, which expresses α-phase and just in-between the zones and at the boundary of patches, β-phase was formed. By varying the cutting speed, thickness of the segmented chips was changed. These adiabatic shear bands concede to huge amount of heat absorbed at the surface of segmented chip and saw teeth like structure was produced on the back side of chips due to bulging of adiabatic shearing.

The table given below shows the calculation of geometric parameters with respect to machining parameters for uncoated tool chips.

Table 10: Calculation of geometric parameters with respect to machining parameters for uncoated tool chips mechanism.

UNCOATED TOOL CHIPS							
Sr No	***f*** ***mm/rev***	***V_c*** ***mm/min***	***t_o***	***h_p*** ***mm***	***h_v*** ***mm***	***θ'***	***P_c*** ***mm***
1	0.16	50000	0.16	0.26	0.13	42.39	0.05
2	0.16	70000	0.16	0.27	0.14	41.05	0.05
3	0.16	150000	0.16	0.40	0.15	44.88	0.05

The calculations of all the geometric parameters for single coated and multi-coated tool chips are presented in the below table.

Table 11: Calculation of geometric parameters with respect to machining parameters for single-coated tool chips mechanism.

SINGLE COATED TOOL CHIPS							
Sr No	***f*** ***mm/rev***	***V_c*** ***mm/min***	***t_o***	***h_p*** ***mm***	***h_v*** ***mm***	***θ'***	***P_c*** ***mm***
1	0.16	50000	0.16	0.24	0.12	45.66	0.05

2	0.16	70000	0.16	0.24	0.13	44.25	0.05
3	0.16	150000	0.16	0.37	0.15	46.13	0.06

Primarily, processing parameters and type of coatings influences on the geometric parameters as clearly shown in the given table:

Table 12: Calculation of geometric parameters with respect to machining parameters for multi-coated tool chips mechanism.

MULTI -COATED TOOL CHIPS							
Sr No	***f*** ***mm/rev***	V_c ***mm/min***	t_o	h_p ***mm***	h_v ***mm***	θ'	P_c ***mm***
1	0.16	50000	0.16	0.21	0.12	46.63	0.06
2	0.16	70000	0.16	0.21	0.12	45.70	0.06
3	0.16	150000	0.16	0.36	0.14	47.00	0.06

During the machining, chips are formed by the plastic deformation i.e. shear deformation of the workpiece. Formation of shear angle is at the shear plane side and mathematically, it can be calculated by the equation given below [26];

$$\boldsymbol{\Phi} = \frac{\pi}{2} - \theta'$$

On the other hand, Segmentation ratio or Degree of segmentation (**Gs),** Chip segmentation frequency ($\mathbf{f_{cs}}$), equivalent deformed chip thickness ($\mathbf{t_c}$), Chip thickness ratio (**r**), Chip shrinkage or reduction coefficient (**1/r**), would be calculated from the formulae given below [26];

$$\mathbf{Gs} = \frac{hp - hv}{hp}$$

$$\mathbf{Fcs} = \frac{Vc}{60 * Pc}$$

$$\mathbf{tc} = hv + \frac{hp - hv}{2}$$

A total of 9 samples was analyzed means 3 samples of uncoated chips, others 3,3 samples were single coated and multi-coated tool chips, calculating each geometric parameter thrice from ImageJ software in order to measure the geometry of parameters accurately. Then, incorporate these values in the above formulae to achieve better results.

On the other hand, two important ratios, i.e. Chip thickness ratio (**r**), Chip shrinkage or reduction coefficient (**1/r**) were calculated, The equations are;

$$\mathbf{r} = \frac{to}{tc}$$

$$\mathbf{r}' = \frac{1}{r}$$

Where $\mathbf{t_o}$ is actually undeformed chip thickness, i.e. feed of 0.16 mm, $\mathbf{t_c}$ denotes equivalent deformed chip thickness, which is calculated by the above mentioned equation. Due to increase of machining speed, cutting zone exhibits high heat generation at the shear zones, thus, resulting reduction in height of peaks, in the meanwhile the instability of shear was also increased.

Table 13: Calculation of response parameters with the help of geometric variables

UNCOATED TOOL CHIPS						
Sr No	**Φ**	**G_s**	**t_c (mm)**	**f_{cs} (Hz)**	**r**	**r'**
1	47.61	0.50	0.20	18040.25	0.81	1.24
2	48.95	0.50	0.21	24763.16	0.78	1.29
3	45.12	0.62	0.28	46983.65	0.58	1.72
	SINGLE COATED TOOL CHIPS					
Sr No	**Φ**	**G_s**	**t_c (mm)**	**f_{cs} (Hz)**	**r**	**r'**

1	44.34	0.48	0.18	16538.99	0.89	1.13
2	45.75	0.47	0.19	22661.20	0.86	1.16
3	43.87	0.60	0.26	44543.43	0.61	1.63

MULTI COATED TOOL CHIPS						
Sr No	**Φ**	**G_s**	**t_c (mm)**	**f_{cs} (Hz)**	**r**	**r'**
1	43.37	0.43	0.16	13393.55	0.98	1.02
2	44.30	0.43	0.17	20817.35	0.97	1.04
3	43.00	0.61	0.25	41700.03	0.65	1.54

4 CHAPTER 04

4.1 Results and discussion:

4.1.1 Comparison and analysis of Ra:

Earlier sections describe the calculation of surface roughness with respect to uncoated, single and multi-coated inserts. In this section, the effect of surface roughness will analyze and discuss on the basis of graphical approach.

The graphical analysis of the fluctuation of roughness values corresponding to Type A, B, C cutting speed is shown in the figures below;

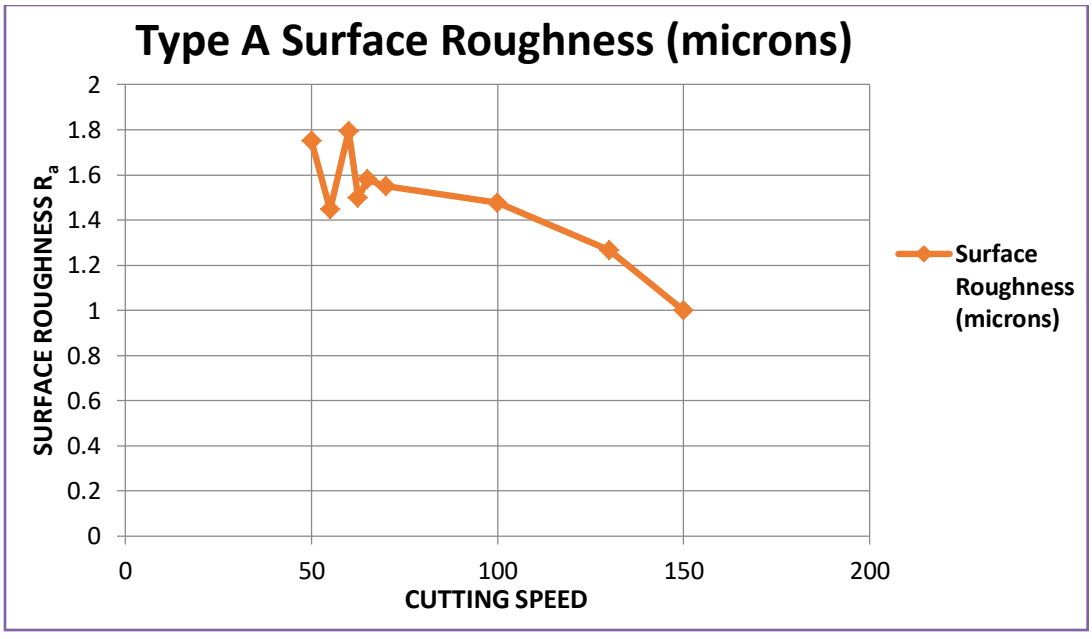

Figure 24: Line Graph for Cutting Speed vs Type A Ra

Generally, for increasing the spindle speed, better surface finish would achieve and the value of surface waviness is decreased. On the other hand, due to high heat generation, the tool deteriorates more. By increasing the nose radius, the value of surface roughness increases.

During the machining, the serrated chips adhere on the tooltip and deteriorate the cutting edge. Thus, by considering all these factors, the variation in roughness value occurs.

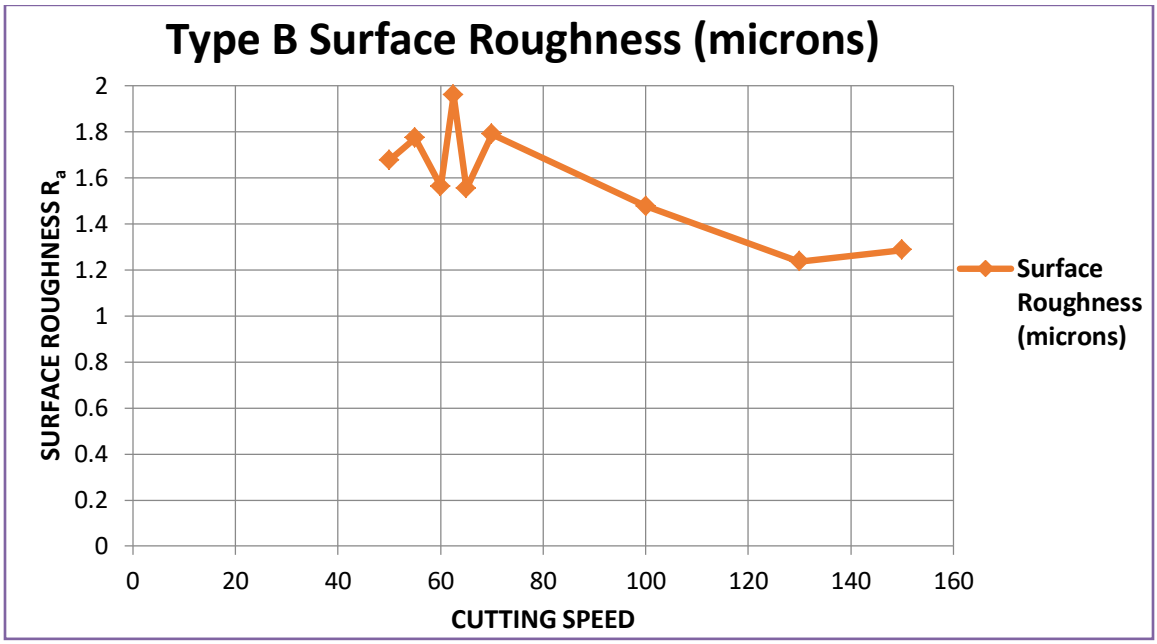

Figure 25: Line Graph for Cutting Speed vs Type B Surface Roughness

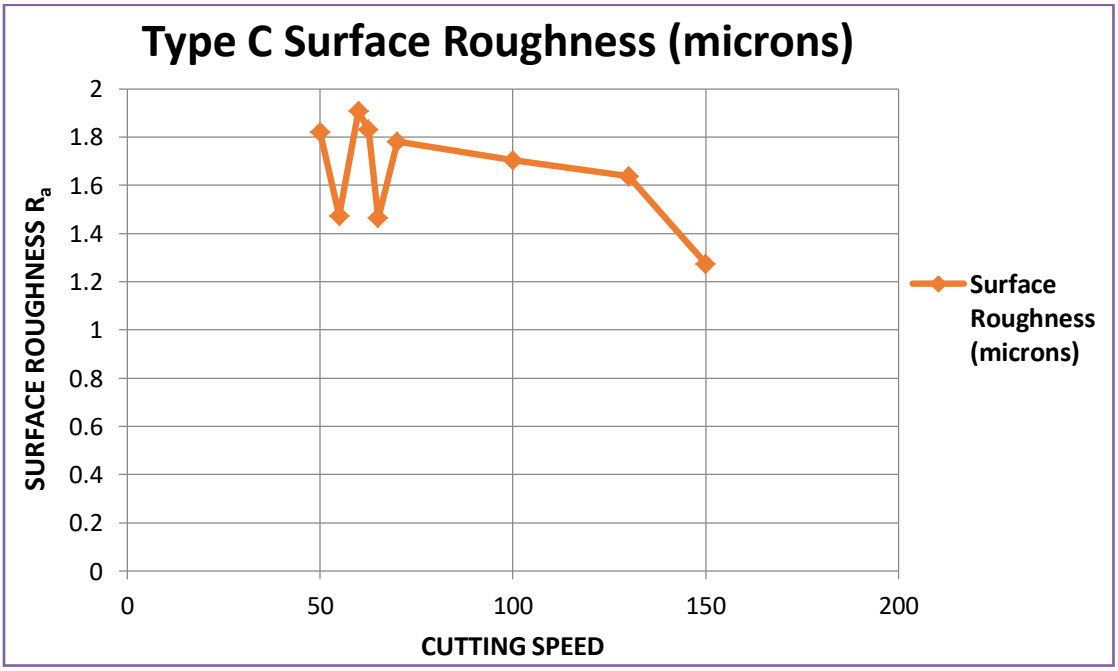

Figure 26: Line Graph for Cutting Speed vs Type C Ra

4.1.2 Comparison of Uncoated, Single and Multi Coated Surface Roughness vs Cutting speed:

The given comparison shows the fluctuations in the average value of Ra with spindle speed and types of coatings. For the cutting speeds of 50 and 55 m/min, it is clearly shown that the surface roughness of uncoated and multi-coated inserts had decreased significantly from 1.75 to 1.44 microns and 1.82 to 1.47 microns respectively, because the cutting speed was dominant in this interval but in case of single coated tools, the value of surface roughness would be gradually increased from 1.67 to 1.77 microns.

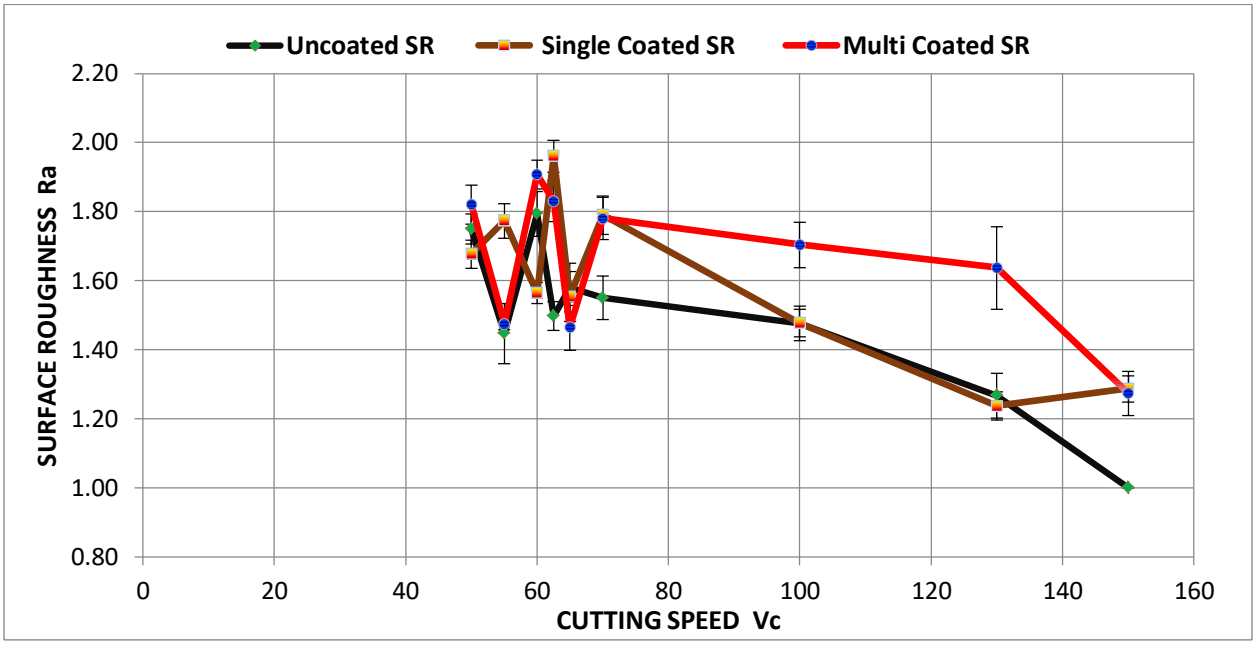

Figure 27: Line graph comparison of uncoated, Single and Multi Coated Ra w.r.t Vc

When moved from cutting speed of 60 and 62.5 m/min, the trend was almost the same for uncoated inserts as for the previous two experiments and single tools gave higher roughness value of 1.56 then reached to maximum of 1.96 microns because of high heat generation and reduction in contact surface area between the coated insert and work piece material but for multi-coated tools, the surface roughness were increased abruptly when moved from 55 to 60 m/min

then it would drop off from 1.90 to 1.83 microns for the third and fourth interval of spindle speed. When machining of this type of alloy with these coatings, it exhibits high temperature generation at the primary and secondary zone of tool-work piece interface by varying the cutting speed [27]. So, at the elevated temperatures, Thermal stability such as hardness and wear resistivity was the major challenge for TiAlN and CrAlN coatings [24].

Last five experiments clearly shown in the figure that there would be gradually decreasing the roughness value and reached with minimum of 1.00 microns. For single coated surface roughness, the SR value first increased for the 5th and 6th experiment then suddenly drop off from 1.79 to 1.47 and at the end achieved 1.28 microns. The SR value of multi-coated inserts suddenly dropped from 1.83 to 1.46 microns at a cutting speed of 62.5 and 65m/min. When moved from 70 to 150m/min, the surface roughness shifted to be decreased and at the end reaches to lower value of 1.27 microns. The main reason for this type of behavior in coated inserts was due to reduction of contact surface area while machining, thus reduces the sharpness of the coated inserts, high heat generated between the tool-work piece interface and thermal conductivity of CrAlN had a decreasing trend, when the temperature went to 200^{o}C or more. That's why, multi-coated inserts gave more SR value as compared to other type of inserts [24]. Another important aspect was the fluctuation of coefficient of friction due to high heat generation and reduction of contact surface area, thus results adhesion of chips at the tool tip interface. Adhesive chips causes variation in cutting forces and induces high stress upon the cutting inserts. Thus, for higher values of cutting speed, this factor is more dominant in multi-coated tools.

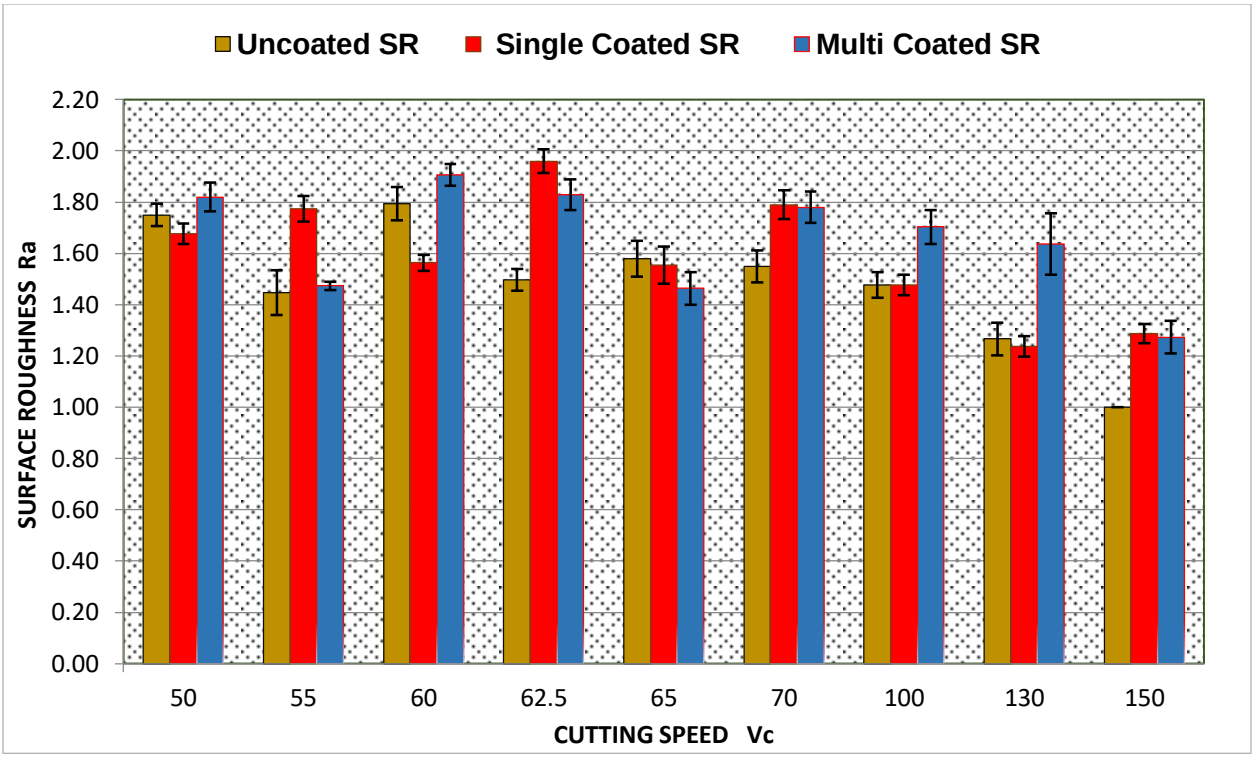

Figure 28: Bar graph comparison of uncoated, Single and Multi Coated Surface roughness vs Cutting speed

Therefore, by increasing the speed, roughness value is decreased and achieves better surface finish and tool deteriorates more in lower values of spindle speed. Tool wear and cutting speed is inversely proportional to each other. Although. Coated inserts have increased the life of cutting inserts due to less deterioration of the tool. But, Ra value is increased because of reduction in contact surface area of coated inserts and the material and this results in reduction of tool-edge sharpness [28].

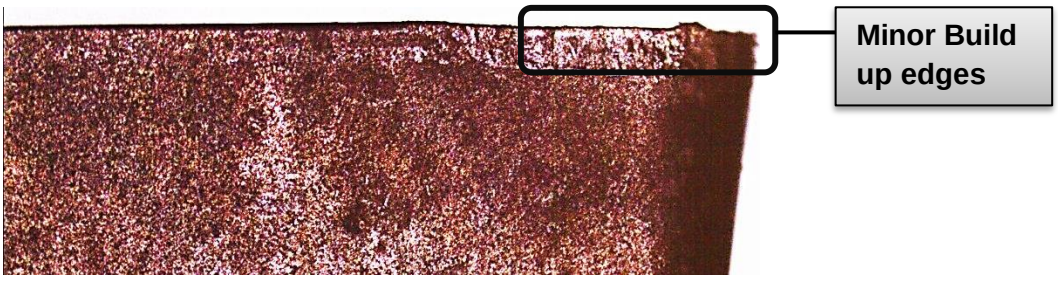

Figure 29: Optical microscopy of uncoated inserts with minimum BUE's

During the experimentation and optical microscopy of the coated and uncoated inserts, it was analyzed that higher wear materials were accumulated at the cutting nose of single and multi-coated inserts as compared to uncoated inserts. The reason behind it that the generated heat weas difficult to transfer [29].

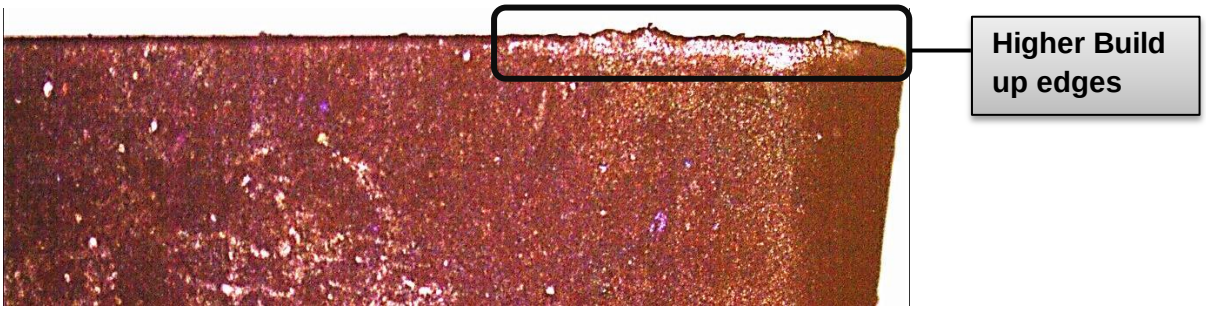

Figure 30: Optical microscopy of single-coated inserts with higher BUE's

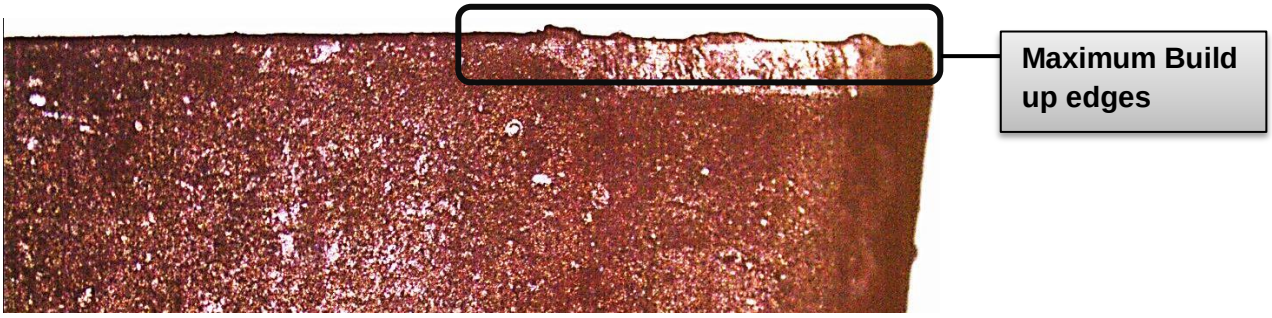

Figure 31: Optical microscopy of multi-coated inserts with maximum BUE's

This difficulty to transfer heat results increases the ductility and due to this, cutting chips was adhered upon the tool-chip interface. This buildup edges causes the increment of cutting forces and results high value of surface roughness in single and multi-coated inserts.

4.1.3 Cutting Time Analysis:

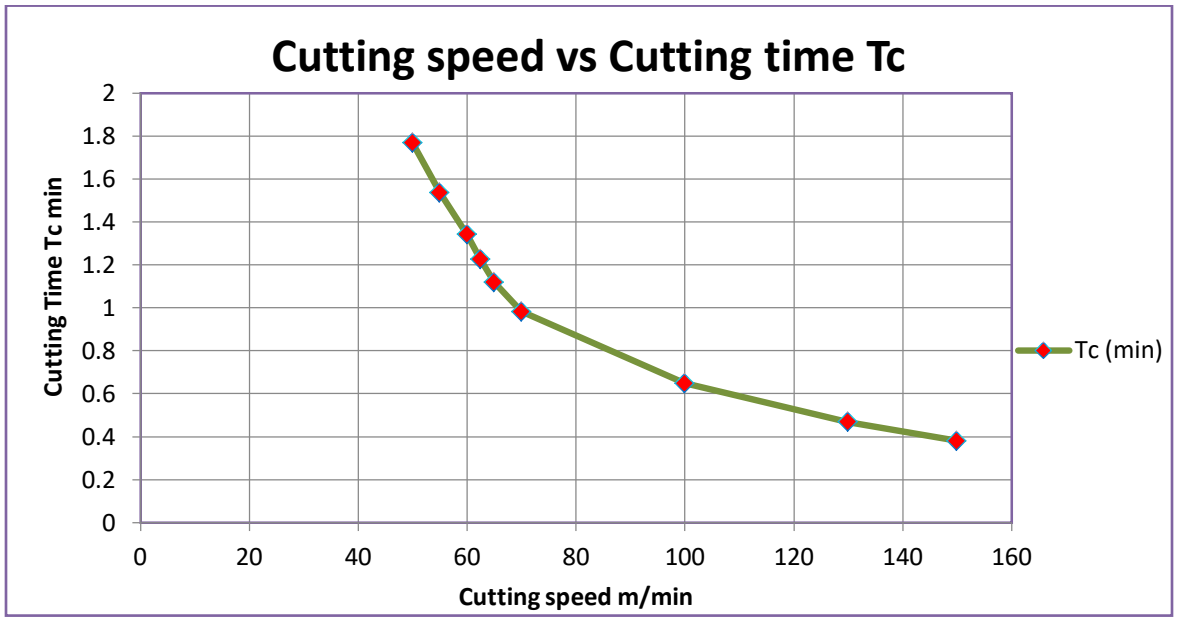

Figure 32: Cutting speed vs Cutting time

The trend of cutting time and cutting speed has an adverse effect. The graph demonstrates that, with the cutting speed of 50m/min the length of active tool engagement is maximum means that the first experiment takes more time to remove the material, i.e. 1.76 min. There would be gradually decreasing the behavior of cutting time, for extreme cutting speed values and at the end of 150 m/min, the length of active tool engagement would reach to lowest value which is 0.37min.

4.1.4 Chips Characterization with Geometric parameters:

In the ImageJ software, the calculations of chips geometrical factors and calculation of all the response variables, graphical technique and subsequent analysis were carried out to check and analyze the behavior of the response variables and how the experimental trend varies with respect to machining parameters and tool coating.

Certain trends were discussed and analyze that how they were varied with the processing parameters. The given figure explains the trend of maximum height value as a function of V_c (m/min). Overall, the trend was increasing because of directly proportional to chip thickness and segmented ratio respectively, with respect to cutting speeds.

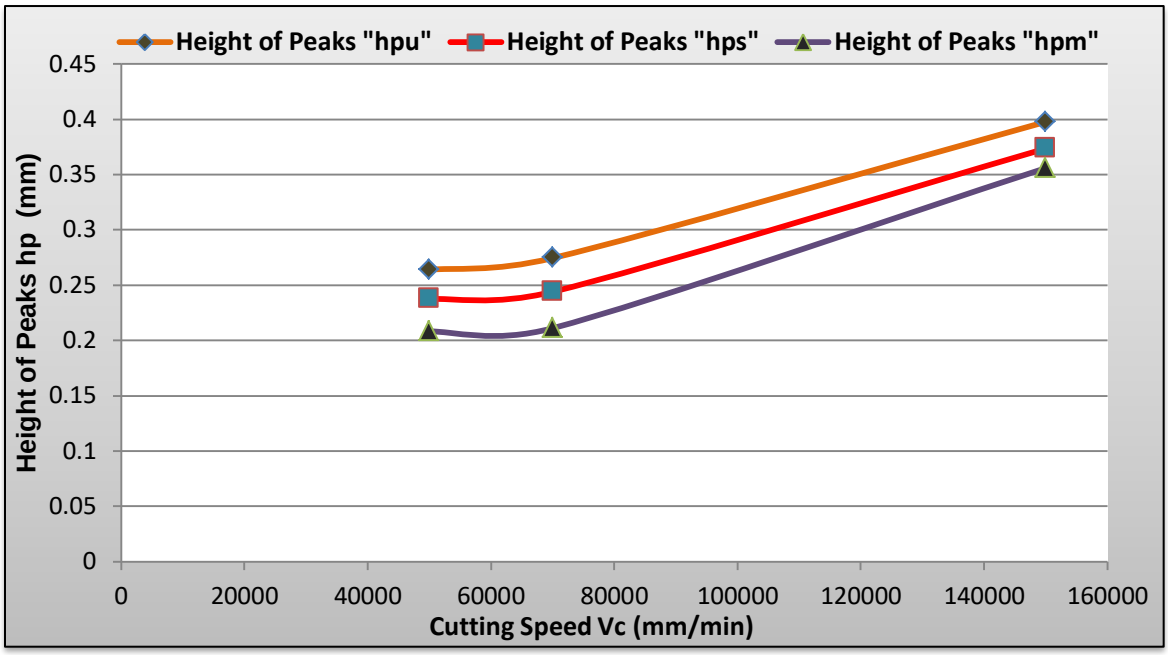

Figure 33: Height of peaks with different coating vs Cutting Speed Vc where h_{pu}, h_{ps}, h_{pm} are the uncoated, single and multi-coated height of peaks.

Specifically, with a speed range from 50 to 70 m/min, there was clearly a normal and increasing trend of peak heights for uncoated, single and multi-coated chips morphology. When moved from low to high cutting speed, i.e. 70 to 150m/min, height of peak trends were increasing linearly for all types of coated chips, but the uncoated chip had reached to maximum height value of 0.3977 mm and single-coated chip was at lower values of h_p. Overall, the least peak height value was 0.2081 mm for the multi-coated chip.

On the other hand, the trend was linearly increased for the height of valleys. For low and high cutting speeds, the same trend was observed for all the chips and reaches to maximum value of

0.15311 mm at a cutting speed of 150 m/min for uncoated chip morphology. This trend is almost similar to the deformed chip thickness because it is directly proportional to height of peaks and valleys.

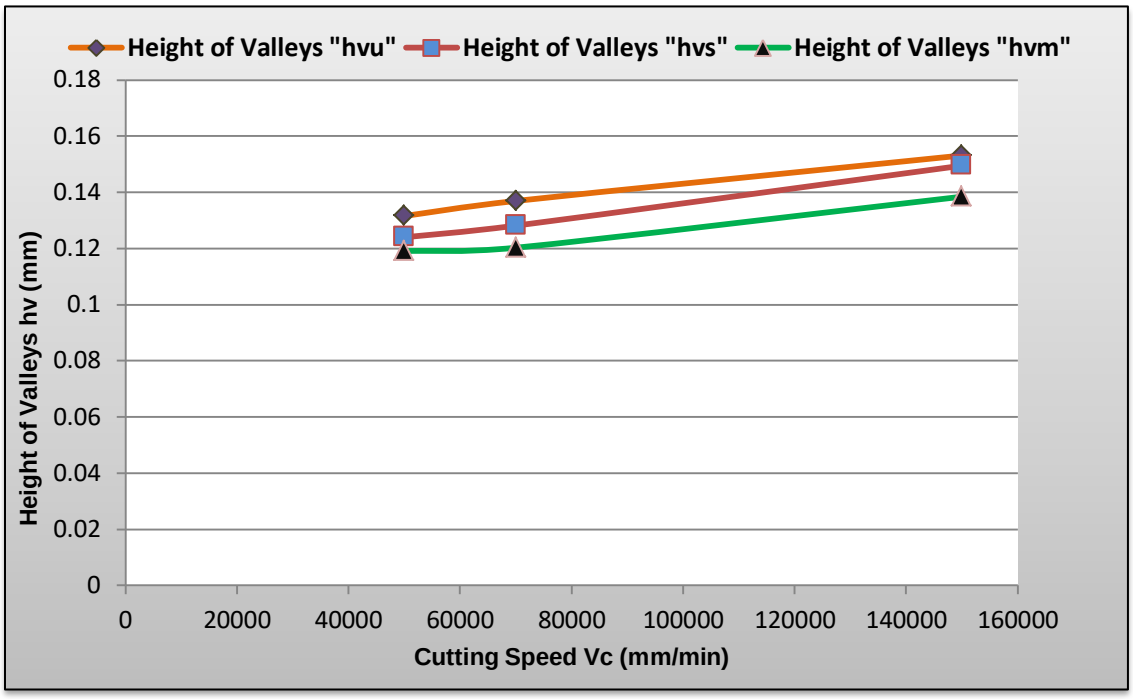

Figure 34: Height of valley with different coating as a function of Cutting Speed Vc where h_{vu}, h_{vs}, h_{vm} are the uncoated, single and multi-coated height of peaks.

Cutting speed also influence on the segmented portion of chip structure, higher the cutting speeds will increase the thermal softening of the titanium alloy. This segmentation ratio will affect and enhance the cracks initiation and propagation by lowering the spindle speed. Segmentation ratio depends upon the height of peak and valley and trend is almost similar to height of peaks fluctuation except at the cutting speed of 150 m/min. At low cutting speeds, there was a constant behavior of segment ratio and multi-coated chips morphology exhibits the least value of segmented proportion which was 0.4277 as compared to other coated chip characteristics. Uncoated chip structure leads to a maximum ratio of segmentation, i.e. 0.61503 at higher cutting speed of 150 m/min with the comparison of single and multi-coated chips ratio.

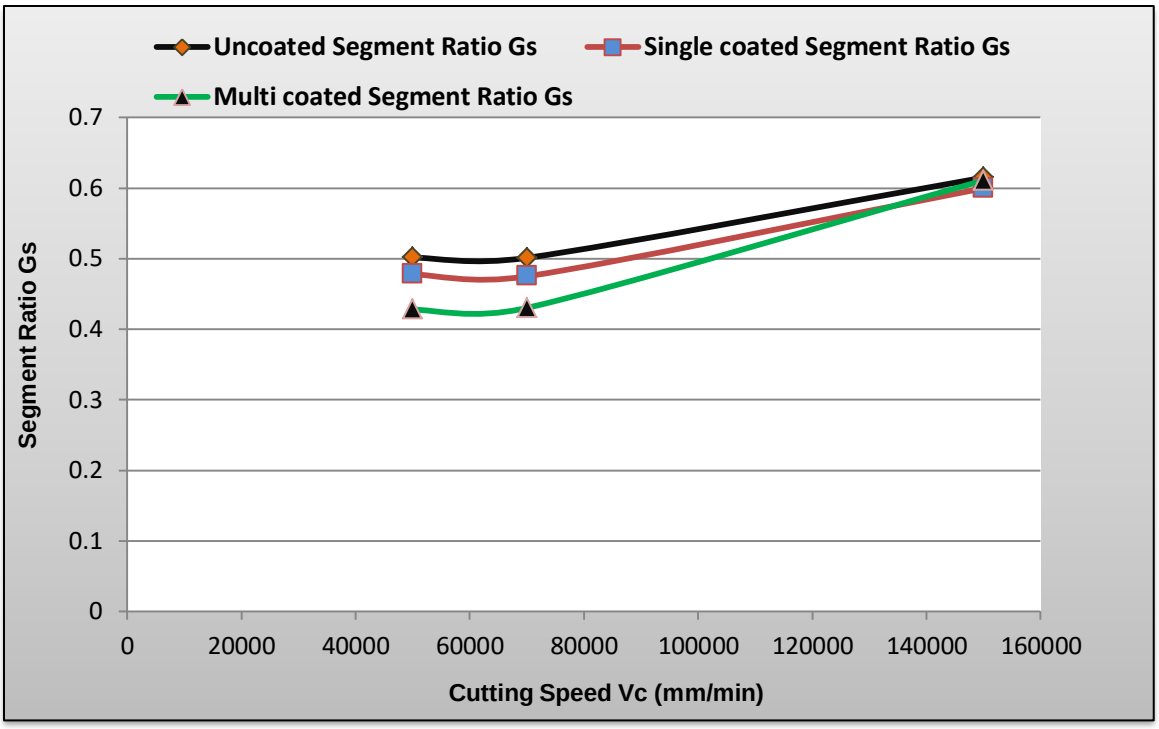

Figure 35: Segment ratio with different coating as a function of Cutting Speed V_c

Equivalent deformed chip thickness surely depends upon the type of coating used and machining parameters. In the given figure, the trend resembles with the height of peak behavior. Overall, the uncoated chips morphology showed a linearly higher trend compared with other type of coating because plastic deformation of the chips and their microstructure directly depends the heat generated at the tool chip interface and the chemical reaction between the tool and the chips. Comprehensively, higher deformed chip thickness was achieved for uncoated chips and multi-coated chip structure had least equivalent deformed chip thickness for all the cutting speed and other parameters were kept constant.

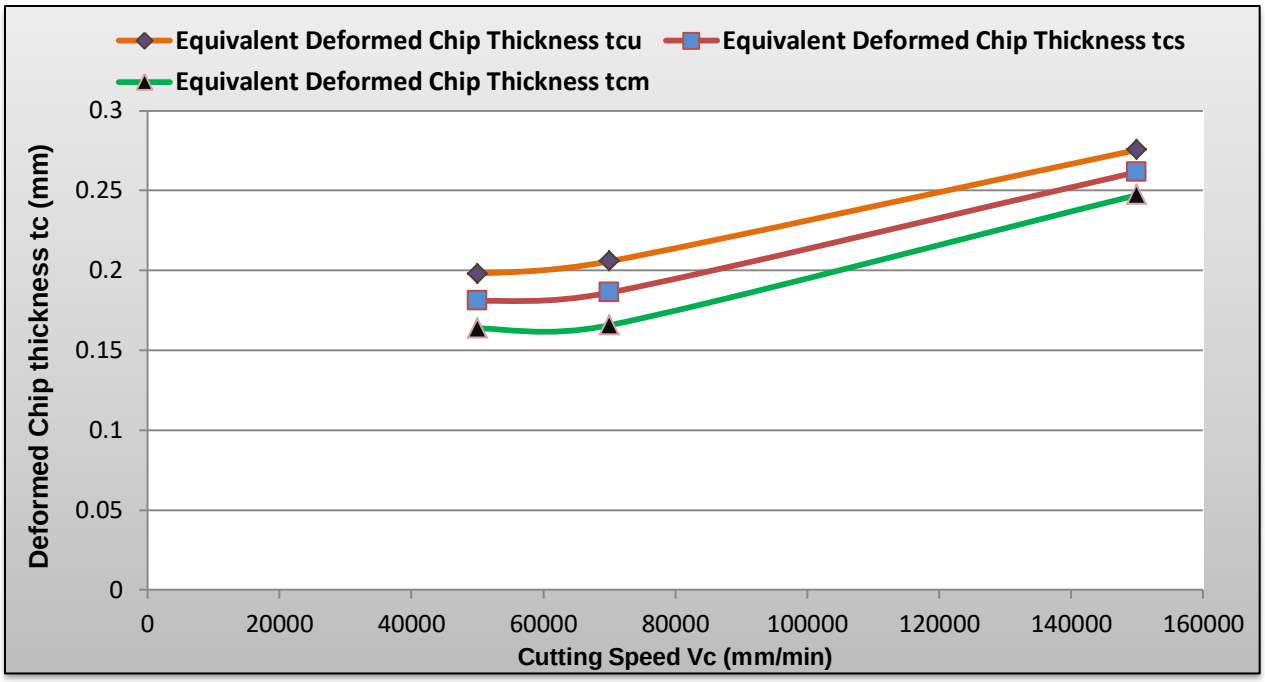

Figure 36: Deformed chip thickness with different coating as a function of Cutting Speed V_c where t_{cu}, t_{cs}, t_{cm} are the uncoated, single and multi-coated equivalent deformed chip thickness.

According to Stabler's theory, the range of shear angle was from 35° to 44° for orthogonal machining of Ti-6Al-4V [30]. For the cutting speeds range from 50 to 150 m/min, irregular or distributed results was observed. Shear deformation was occurring in the shear direction of the tool-chip interface. In my case, with the speed range of 50 to 70 m/min, there was a slighter increasing behavior of shear angle and gradually declining trend was perceived due to higher plastic or shear deformation, when it goes to 150 m/min for uncoated chip morphology. As, in the figure given below, the single and multi-coated coated chips shear deformation had a linearly increasing trend at the start, then smoothly decreased at the end, which shows that chips deformed in a regular manner and attained almost 43.86° and 43° at the cutting speed of 150 m/min. This means that single and multi-coating gave effective thermal barrier because of lower thermal conductivity.

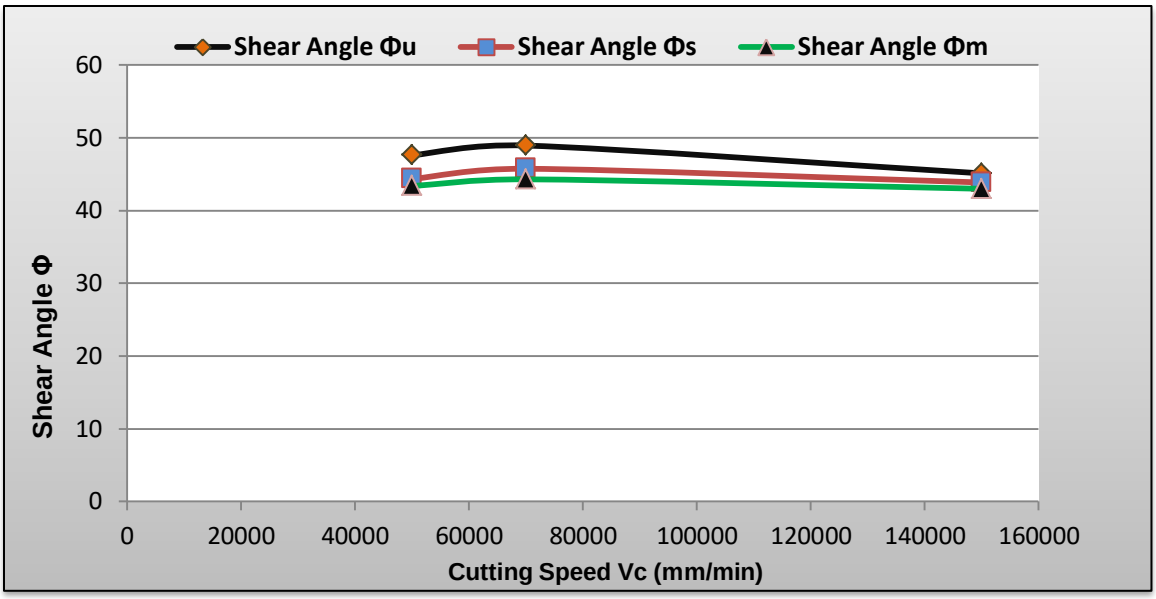

Figure 37: Shear angle Φ with different coating as a function of Cutting Speed Vc where Φ_u, Φ_s, Φ_m are the uncoated, single and multi-coated shear angles.

Chip thickness ratio basically the ratio of equivalent un-deformed chip thickness and deformed chip thickness and it is also called shrinkage factor. In my case, Un-deformed chip thickness is basically the feed-rate which is 0.16 mm/rev [26].

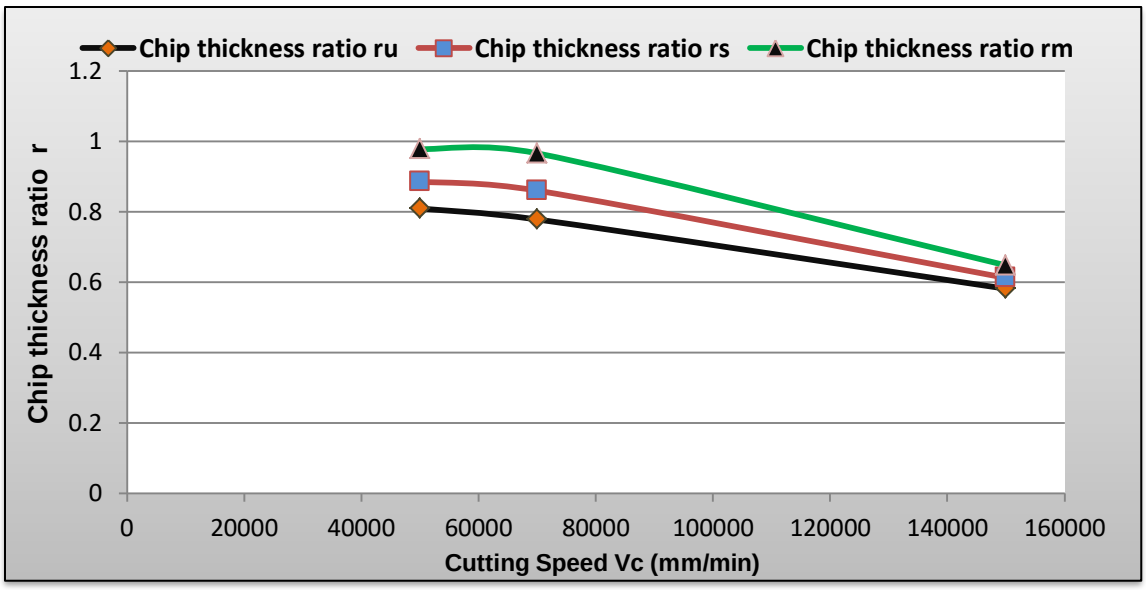

Figure 38: Chip thickness ratio 'r' with different coating as a function of Cutting Speed Vc where r_u, r_s, r_m are the uncoated, single and multi-coated chip thickness ratios.

The deformed chip thickness always greater than the thickness before cutting operation because the chip is separate from work piece by the action of cutting tool, which undergoes severe plastic deformation. This means the chip could not return to original dimensions, hence there shall always be strained associates with it. So, separated chip will have larger dimension than uncut chip thickness. In multi-coating chips morphology, chip thickness ratio had a linearly decreasing trend for low and high speed machining, and reaches to 0.6473 at the end. For single and uncoated chips, the behavior remains the same and uncoated chips leads to minimum value of 'r' for the cutting speed of 150 m/min which is 0.5809.

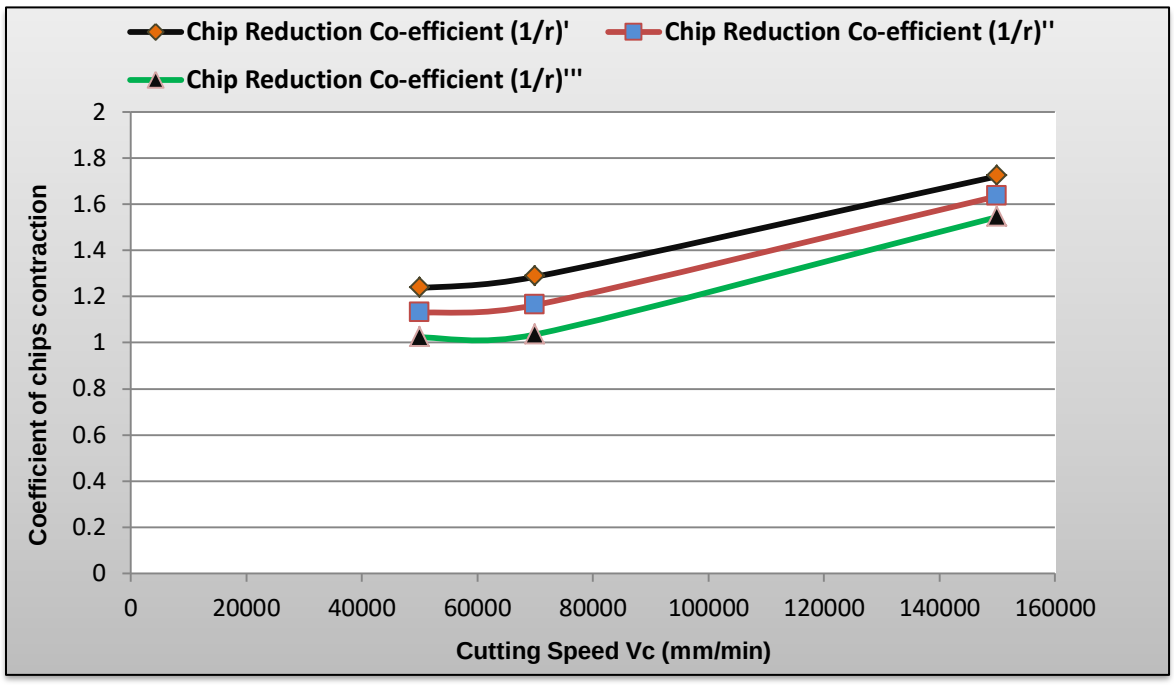

Figure 39: Chip reduction coefficient '1/r' with different coating as a function of Cutting Speed V_c where (1/r)', (1/r)'', (1/r)''' is the uncoated, single and multi-coated coefficient of chips contraction.

Coefficient of chip reduction is basically the inverse of the chip thickness ratio and it is also known as coefficient of chips contraction and its range must have greater than 1. It depends upon the nose radius and the trend of cutting angle, when the cutting angle increase (means that positive rake angle must have a smaller value), then the contraction of chips will increase. On the

other hand, when the radius of tool tip increases the coefficient of the chip reduction would must increase. In my case, chips deformation and tool wear were maximum for uncoated chips, so, coefficient of chip contraction had increased in a regular behavior and multi-coated chips had a least chip reduction coefficient because of the layer of TiAlN and CrAlN coating, in order to avoid shear deformation.

5 CHAPTER 05

5.1 Conclusion and Recommendation:

In this research, I have analyzed and compare the behavior of surface roughness with the performance of uncoated, PVD single and multi-coated inserts of tungsten carbide inserts. Detailed experiments were carried out by selecting the processing parameters from the wear rate map. It was concluded that the coated inserts gave more value of surface roughness as compared to uncoated inserts. An assessment conducted that in single and multi-coated inserts, the contact surface area was reduced, which results, reduction in cutting edge sharpness. Secondly, during the machining, the fluctuation of coefficient of friction due to high heat generation and reduction of contact surface area, which causes adhesion of chips at the tool tip interface. Adhesive chips were caused variation in cutting forces and induces high stress upon the cutting inserts. These factors were more dominant in multi-coated tools for high values of cutting speed.

Coated inserts have increased the life of cutting inserts due to less tool wear. However, the value of surface roughness would grow up because more wear materials were accumulated on the surface of cutting edge for single and multi-coated inserts as compared to uncoated inserts. This buildup edges caused cutting forces to be increased and enhanced the value of Ra in single and multi-coated inserts.

In the meanwhile, I have also investigated the geometrical parameters, morphology and microstructure of cutting chips with respect to cutting speed and type of inserts used. The collected chips had sawtooth like structure with chip waviness to be smoother on the outer surface which was analyzed under the optical microscope. The microstructure of the segmented chips was observed and deformed grains, shear zones with crack initiation were highlighted. By

increasing the cutting speed V_c, adiabatic shear bands, shear zones and deformed grains in specified segmented regions were more noticeable.

For changing the cutting speed and feed, various geometric parameters of the segmented chips and their response variables were measured and calculated. An Investigation was conducted by comparing these parameters with different types of coating. As, by increasing the cutting speed, almost linearly increasing trend in the height of peaks (h_p), height of the valley (h_v), equivalent deformed chip thickness and segmentation ratio. Uncoated chips were dominant as compared to coated chips because plastic deformation of the chips and their microstructure directly depends on the heat generated at the tool chip interface and the amount of tool wear. The deformed chip thickness (t_c) had an identical trend as that of h_p and h_v because of direct proportionality. For the cutting speeds range from 50 to 150 m/min, irregular or distributed results of shear angle were observed. More shear deformation was carried out along the shear direction of uncoated chips as compared to coated chips morphology.

Results for the chip thickness ratio and coefficient of chips contraction had an adverse effect. Chips deformation and tool wear were maximum for uncoated chips, so, coefficient of chip contraction had increased in a regular manner and multi-coated chips had a least chip reduction coefficient because of the layer of TiAlN and CrAlN coating, in order to avoid shear deformation. Multi-coated chips were dominant in chip thickness ratio and its trend was linearly decrease by increasing the cutting speed.

6 References

1. Ekinovic, S. and E. Begovic, *An approach to determine transition area from conventional to high-speed machining by means of chip shape analysis.* Archives of Materials Science, 2007. **28**(1-4): p. 35-39.
2. Donachie, M.J., *Titanium: a technical guide*. 2000: ASM international.
3. Bridges, P. and B. Magnus, *Manufacture of titanium alloy components for aerospace and military applications.* Research and Technology Organization, France, 2001.
4. Ezugwu, E., J. Bonney, and Y. Yamane, *An overview of the machinability of aeroengine alloys.* Journal of materials processing technology, 2003. **134**(2): p. 233-253.
5. Donachie Jr, M.J., *Titanium. A Technical Guide. Metals Park, OH: ASM International*. 1988, ISBN 0-87170-309-2.
6. Donachie, M. *Titanium: a technical guide, Metals Park, OH 44073: Asm*. 1988. Intl.
7. Jaffery, S. and P. Mativenga, *Assessment of the machinability of Ti-6Al-4V alloy using the wear map approach.* The International Journal of Advanced Manufacturing Technology, 2009. **40**(7-8): p. 687-696.
8. Rahman, M., Z.-G. Wang, and Y.-S. Wong, *A review on high-speed machining of titanium alloys.* JSME International Journal Series C Mechanical Systems, Machine Elements and Manufacturing, 2006. **49**(1): p. 11-20.
9. Revankar, G.D., et al., *Analysis of surface roughness and hardness in titanium alloy machining with polycrystalline diamond tool under different lubricating modes.* Materials Research, 2014. **17**(4): p. 1010-1022.
10. Zain, A.M., H. Haron, and S. Sharif, *Simulated annealing to estimate the optimal cutting conditions for minimizing surface roughness in end milling Ti-6Al-4V.* Machining Science and Technology, 2010. **14**(1): p. 43-62.
11. Selvakumar, S., R. Ravikumar, and K. Raja, *Implementation of response surface methodology in finish turning on titanium alloy Gr. 2.* European Journal of Science and Research, 2012. **81**(3): p. 436-445.

12. Ramesh, S., L. Karunamoorthy, and K. Palanikumar, *Measurement and analysis of surface roughness in turning of aerospace titanium alloy (gr5).* Measurement, 2012. **45**(5): p. 1266-1276.
13. Dass, K. and S. Chauhan, *Machinability study of titanium (Grade-5) alloy using design of experiment technique.* Engineering, 2011. **3**(06): p. 609.
14. Ezugwu, E. and Z. Wang, *Titanium alloys and their machinability—a review.* Journal of materials processing technology, 1997. **68**(3): p. 262-274.
15. Ribeiro, M., M. Moreira, and J. Ferreira, *Optimization of titanium alloy (6Al–4V) machining.* Journal of materials processing technology, 2003. **143**: p. 458-463.
16. Yang, X. and C. Richard Liu, *Machining titanium and its alloys.* Machining Science and Technology, 1999. **3**(1): p. 107-139.
17. Ezugwu, E., *High speed machining of aero-engine alloys.* Journal of the Brazilian society of mechanical sciences and engineering, 2004. **26**(1): p. 1-11.
18. Caliskan, H., P. Panjan, and C. Kurbanoglu, *Hard Coatings on Cutting Tools and Surface Finish. Reference Module in Materials Science and Materials Engineering*. 2016: Elsevier Science Direct.
19. Calamaz, M., D. Coupard, and F. Girot, *A new material model for 2D numerical simulation of serrated chip formation when machining titanium alloy Ti–6Al–4V.* International Journal of Machine Tools and Manufacture, 2008. **48**(3-4): p. 275-288.
20. Maity, K. and S. Pradhan, *Study of Chip Morphology, Flank Wear on Different Machinability Conditions of Titanium Alloy (Ti-6Al-4V) Using Response Surface Methodology Approach.* International Journal of Materials Forming and Machining Processes (IJMFMP), 2017. **4**(1): p. 19-37.
21. Ahsan, K.B., A.M. Mazid, and G.K. Pang, *Morphological investigation of Ti-6Al-4V chips produced by conventional turning.* International Journal of Machining and Machinability of Materials, 2016. **18**(1-2): p. 138-154.
22. Priyadarshini, A., S.K. Pal, and A.K. Samantaray, *A finite element study of chip formation process in orthogonal machining*, in *Dynamic Methods and Process Advancements in Mechanical, Manufacturing, and Materials Engineering*. 2013, IGI Global. p. 197-225.

23. Khorasani, A.M., M.R.S. Yazdi, and M.S. Safizadeh, *Analysis of machining parameters effects on surface roughness: a review.* International Journal of Computational Materials Science and Surface Engineering, 2012. **5**(1): p. 68-84.
24. Kalss, W., et al., *Modern coatings in high performance cutting applications.* International Journal of Refractory Metals and Hard Materials, 2006. **24**(5): p. 399-404.
25. Jaffery, S.H.I. and P.T. Mativenga, *Wear mechanisms analysis for turning Ti-6Al-4V—towards the development of suitable tool coatings.* The International Journal of Advanced Manufacturing Technology, 2012. **58**(5-8): p. 479-493.
26. Sánchez Hernández, Y., et al., *Experimental Parametric Relationships for Chip Geometry in Dry Machining of the Ti6Al4V Alloy.* Materials, 2018. **11**(7): p. 1260.
27. Ballal, Y.P., M.M. Khade, and A.R. Mane, *Comparison of Performance of Coated Carbide Inserts with Uncoated Carbide Inserts in Turning Gray Cast Iron.* International Journal of Mechanical Engineering & Technology (IJMET), 2013. **4**(2): p. 392-400.
28. Bayraktar, S., et al. *A Performance Comparison Study of Uncoated and TiAlN Coated Carbide End Mill on Machining of the Al-35Zn Alloy*. in *IOP Conference Series: Materials Science and Engineering*. 2018. IOP Publishing.
29. Übeyli, M., et al., *Study on performance of uncoated and coated tools in milling of Al–4% Cu/B4C metal matrix composites.* Materials Science and Technology, 2007. **23**(8): p. 945-950.
30. Grzesik, W., *Advanced machining processes of metallic materials: theory, modelling and applications*. 2008: Elsevier.

7 Appendices

7.1 Appendix A1

A total of 27 experiments is performed. The table shown below describes the design of experiments;

Table 14: Design of experiments

UNCOATED EXPERIMENTS							
Sr.No	**Feed**	**Speed"V" m/min**	**Coating Thickness (Nil)**	**SR1 "Ra" microns**	**SR2**	**SR3**	**Average SR**
1	0.16	50	Uncoated	**1.7**	**1.77**	**1.78**	**1.75**
2	0.16	55	Uncoated	**1.52**	**1.35**	**1.47**	**1.45**
3	0.16	60	Uncoated	**1.79**	**1.86**	**1.73**	**1.79**
4	0.16	62.5	Uncoated	**1.51**	**1.53**	**1.45**	**1.50**
5	0.16	65	Uncoated	**1.66**	**1.53**	**1.55**	**1.58**
6	0.16	70	Uncoated	**1.62**	**1.5**	**1.53**	**1.55**
7	0.16	100	Uncoated	**1.47**	**1.43**	**1.53**	**1.48**
8	0.16	130	Uncoated	**1.22**	**1.34**	**1.24**	**1.27**
9	0.16	150	Uncoated	**1**	**1**	**1**	**1.00**
SINGLE COATED EXPERIMENTS							
Sr.No	**Feed**	**Speed"V" m/min**	**Coating Thickness (1.5 microns)**	**SR1 "Ra" microns**	**SR2**	**SR3**	**Average SR**
1	0.16	50	TiAlN	**1.67**	**1.72**	**1.64**	**1.68**
2	0.16	55	TiAlN	**1.72**	**1.82**	**1.78**	**1.77**
3	0.16	60	TiAlN	**1.53**	**1.59**	**1.57**	**1.56**
4	0.16	62.5	TiAlN	**2**	**1.91**	**1.97**	**1.96**
5	0.16	65	TiAlN	**1.47**	**1.59**	**1.6**	**1.55**
6	0.16	70	TiAlN	**1.8**	**1.84**	**1.73**	**1.79**
7	0.16	100	TiAlN	**1.47**	**1.44**	**1.52**	**1.48**

8	0.16	130	TiAlN	**1.2**	**1.23**	**1.28**	**1.24**
9	0.16	150	TiAlN	**1.33**	**1.26**	**1.27**	**1.29**
MULTI COATED EXPERIMENTS							
Sr.No	**Feed**	**Speed"V" m/min**	**Coating Thickness (1.5 microns)**	**SR1 "Ra" microns**	**SR2**	**SR3**	**Average SR**
1	0.16	50	TiAlN + CrAlN	**1.77**	**1.88**	**1.81**	**1.82**
2	0.16	55	TiAlN + CrAlN	**1.49**	**1.46**	**1.47**	**1.47**
3	0.16	60	TiAlN + CrAlN	**1.86**	**1.92**	**1.94**	**1.91**
4	0.16	62.5	TiAlN + CrAlN	**1.83**	**1.77**	**1.89**	**1.83**
5	0.16	65	TiAlN + CrAlN	**1.49**	**1.39**	**1.51**	**1.46**
6	0.16	70	TiAlN + CrAlN	**1.81**	**1.71**	**1.82**	**1.78**
7	0.16	100	TiAlN + CrAlN	**1.66**	**1.78**	**1.67**	**1.70**
8	0.16	130	TiAlN + CrAlN	**1.52**	**1.63**	**1.76**	**1.64**
9	0.16	150	TiAlN + CrAlN	**1.31**	**1.2**	**1.31**	**1.27**

7.2 Appendix A2

Experimental details of turning test are shown in the table below;

The formula of spindle speed is;

$$\boldsymbol{RPM} = \frac{Cutting\ Speed\ \times 1000}{\pi \times Diameter}$$

Table 15: Experimental details of turning test

Sr No	Feed mm/rev	Speed "V" m/min	Spindle Speed "N" (RPM)	Diameter "D" (mm)	Depth of cut mm	Linear Length of cut mm
1	0.16	50	353.68	45	1	100
2	0.16	55	407.14	43	1	100
3	0.16	60	465.82	41	1	100

4	0.16	62.5	510.11	39	1	100
5	0.16	65	559.19	37	1	100
6	0.16	70	636.62	35	1	100
7	0.16	100	964.58	33	1	100
8	0.16	130	1334.85	31	1	100
9	0.16	150	1646.43	29	1	100

7.3 Appendix A3

The Material Removal Rates for all the nine machining operations is shown in the table below;

$$\boldsymbol{MRR} = Cutting\ Speed\ \times Feed\ \times Depth\ of\ Cut\ \times 1000$$

Table 16: Calculation of Material Removal Rate

Sr No	Feed mm/rev	Speed "V" m/min	Depth of cut mm	Linear Length of cut mm	Material Removal Rate (mm^3/min)
1	0.16	50	1	100	8000
2	0.16	55	1	100	8800
3	0.16	60	1	100	9600
4	0.16	62.5	1	100	10000
5	0.16	65	1	100	10400
6	0.16	70	1	100	11200
7	0.16	100	1	100	16000
8	0.16	130	1	100	20800
9	0.16	150	1	100	24000

7.4 Appendix A4

Length of Active tool engagement or it is also called cutting time for the rate of material removal.

The formula of cutting time is:

$$\boldsymbol{Tc} = \frac{\pi \times Diameter \times Linear\ length\ of\ cut}{1000 \times Feed\ \times Cutting\ Speed}$$

Table 17: Calculation of length of active tool engagement

Sr No	Feed mm/rev	Speed "V" m/min	Diameter "D" (mm)	Depth of cut mm	Linear Length of cut mm	Tc (min)
1	0.16	50	45	1	100	**1.77**
2	0.16	55	43	1	100	**1.54**
3	0.16	60	41	1	100	**1.34**
4	0.16	62.5	39	1	100	**1.23**
5	0.16	65	37	1	100	**1.12**
6	0.16	70	35	1	100	**0.98**
7	0.16	100	33	1	100	**0.65**
8	0.16	130	31	1	100	**0.47**
9	0.16	150	29	1	100	**0.38**